molecular pharmaceutics

articles

Development of Structure−Lipid Bilayer Permeability Relationships for Peptide-like Small Organic Molecules

Yichen Cao, Tian-Xiang Xiang, and Bradley D. Anderson*

Department of Pharmaceutical Sciences, College of Pharmacy, University of Kentucky, Lexington, Kentucky 40536

Received July 30, 2007; Revised Manuscript Received December 16, 2007; Accepted January 25, 2008

Abstract: Computational methods to estimate passive membrane permeability coefficients of organic molecules, including peptides, would be valuable in understanding various biological processes associated with molecular transport across cell membranes and in reducing the time required for screening developability properties of new drug candidates. This study explores the suitability of fragment-based linear free energy relationships (LFERs) to predict lipid bilayer permeability coefficients and decadiene/water partition coefficients of a set of 47 model permeants. The inclusion of mono-, di-, and tripeptides comprised of glycine, alanine, and sarcosine residues in the database presented added challenges due to the apparent lack of independence of the contribution of the backbone amide residue in peptides to the free energy of transfer ($\Delta(\Delta G^\circ)_{\text{-CONH-}}$) from water to organic solvents or to the bilayer barrier domain. In order to elucidate the impact of neighboring group effects on $\Delta(\Delta G^\circ)_{\text{-CONH-}}$, a series of RGZ glycine (G)-containing peptides having an additional -$NHCH_2CO$- residue compared to their RZ counterparts were synthesized, where R = acetyl (Ac-), 4-carboxymethylphenyl acetyl (CMPA-), or 4-methylphenyl acetyl (MPA-), and Z = -OH, -OMe, -NHMe, or -NMe_2. While variations in R had no significant impact on $\Delta(\Delta G^\circ)_{\text{-Gly-}}$, significant effects of neighboring ($i + 1$) Z substituents at the C-terminus were revealed both in studies of the relative transport of RGZ/RZ compound pairs across DOPC bilayers and partitioning between water and 1,9-decadiene (a bulk solvent with a similar chemical selectivity to the barrier domain of DOPC/eggPC bilayers). The proximity effects decline when the bulk solvent used in partitioning studies is 1-octanol, suggesting a possible role for intramolecular hydrogen bonding in the observed nonadditivity of $\Delta(\Delta G^\circ)_{\text{-CONH-}}$. A new LFER for predicting decadiene/water partition coefficients was developed by including the contributions of polar fragments, total nonpolar surface area of nonpolar fragments, and correction factors to account for the effects of $i + 1$ substituents in peptides on the group contribution of the peptide backbone amide bond to the free energy of transfer. This LFER could be used to predict lipid bilayer permeability coefficients by including an additional term to account for the added influence of molecular size on bilayer permeability.

Keywords: Lipid bilayer permeability; membrane transport; partition coefficients; linear free energy relationships; computational methods; drug absorption; peptides

Introduction

High-throughput screening of drug candidates for pharmacological activity combined with accelerated methods of compound synthesis have increased the number of candidates being evaluated for their developability properties such as solubility, membrane permeability, susceptibility to metabolic enzymes and efflux transporters, etc. Without corresponding high-throughput methods to reliably evaluate such properties, bottlenecks may occur at this stage in the drug development process. Computational methods that enable the prediction of physicochemical properties solely from molecular structure

* To whom correspondence should be addressed. Mailing address: A323A ASTeCC Building, University of Kentucky, Lexington, KY 40506. Tel: 859-218-6536. Fax: 859-257-2489. E-mail: bande2@email.uky.edu.

10.1021/mp700100n CCC: $40.75
Published on Web 03/21/2008

would be invaluable in avoiding delays in the drug development process stemming from the need to assess the developability of large numbers of candidates.[1–4]

The passive permeability coefficient of a given drug molecule across biomembranes is a particularly important physicochemical property-related characteristic because of its role in determining the extent of oral bioavailability and drug access to certain target organs such as the brain. Biomembranes consist of complex assemblies of proteins embedded within a lipid bilayer matrix, including many transmembrane proteins that function as uptake or efflux transporters. Consequently, the accurate prediction of the transport rate of any particular permeant across a given biological membrane will remain a formidable challenge for quite some time.

Nevertheless, significant progress has been made in understanding the permeant structural features that influence passive permeability across lipid bilayers[5–13] and the influence of membrane composition on bilayer selectivity to permeant size and other structural attributes.[11,14–21] For example, previous studies in our laboratories have demonstrated that a fragment-based approach derived from linear free energy relationships (LFERs) can be useful for predicting relative permeabilities of similarly sized permeants having one or more polar functional groups across a variety of liquid crystalline and gel phase bilayers, providing that the functional groups are well isolated from each other.[7,8,13] Such studies have established that the barrier domain within liquid crystalline bilayers resembles relatively nonpolar hydrocarbon solvents such as 1,9-decadiene (for DOPC or egg PC)[8,13] or hexadecane (for DPPC).[19] The goal of the present work is to explore the possibility of extending the fragment-based LFER approach to include more complex molecules such as small peptides containing glycine, alanine, or sarcosine residues in order to predict their transport across liquid crystalline bilayers such as DOPC or egg PC.

Fragment-based LFERs attempt to relate the energetics of solute permeation, membrane adsorption, partitioning, etc., to the individual contributions of molecular fragments (i.e., atoms or functional groups) by assuming that these contributions are both independent and additive regardless of the structure of the overall molecule. While the approach has found wide application for monofunctional compounds and more complex solutes in which polar groups are well-isolated, it has been recognized for many years that simple structure−additivity rules may no longer apply to polyfunctional molecules when two or more polar groups are in close proximity.[22–24] Comparisons of small molecule fragment-based predictions based on the structure−additivity assumption with hydrophobicity or hydropathy scales for peptides

(1) Blake, J. F. Chemoinformatics - predicting the physicochemical properties of "drug-like" molecules. *Curr. Opin. Biotechnol.* **2000**, *11*, 104–107.

(2) Clark, D. E.; Pickett, S. D. Computational methods for the prediction of drug-likeness. *Drug Discovery Today* **2000**, *5*, 49–58.

(3) George, A. The design and molecular modeling of CNS drugs. *Curr. Opin. Drug Discovery Dev.* **1999**, *2*, 286–292.

(4) Stenberg, P.; Luthman, K.; Artursson, P. Prediction of membrane permeability to peptides from calculated dynamic molecular surface properties. *Pharm. Res.* **1999**, *16* (2), 205–12. [published erratum appears in *Pharm Res.* **1999**, *16*, 1324]

(5) Finkelstein, A. Water and nonelectrolyte permeability of lipid bilayer membranes. *J. Gen. Physiol.* **1976**, *68*, 127–135.

(6) Gutknecht, J.; Walter, A. Histamine, theophylline and tryptamine transport through lipid bilayer membranes. *Biochim. Biophys. Acta* **1981**, *649*, 149–154.

(7) Mayer, P.; Xiang, T.-X.; Anderson, B. D. Independence of substituent contributions to the transport of small molecule permeants in lipid bilayers. *AAPS PharmSci* **2000**, *2* (2), 1–13, article 14 (http://www.pharmsci.org/)

(8) Mayer, P. T.; Anderson, B. D. Transport across 1,9-decadiene precisely mimics the chemical selectivity of the barrier domain in egg Lecithin bilayers. *J. Pharm. Sci.* **2002**, *91*, 640–646.

(9) Mayer, P. T.; Xiang, T.-X.; Niemi, R.; Anderson, B. D. A hydrophobicity scale for the lipid bilayer barrier domain from peptide permeabilities: Nonadditivities in residue contributions. *Biochemistry* **2003**, *42*, 1624–1636.

(10) Stein, W. D. Permeability for lipophilic molecules. In *Membrane Transport*; Bonting, S. I., dePont, J. J. H. H. M., Eds.; Elsevier/North-Holland Biomedical: New York, 1981; pp 1–28..

(11) Stein, W. D. *Transport and Diffusion Across Cell Membranes*; Academic Press, Inc.: Orlando, FL, 1986.

(12) Wright, E. M.; Diamond, J. M. Patterns of non-electrolyte permeability. *Proc. R. Soc. Chem. B* **1969**, *172*, 227–271.

(13) Xiang, T.-X.; Anderson, B. D. Substituent contributions to the transport of substituted p-toluic acids in lipid bilayer membranes. *J. Pharm. Sci.* **1994**, *83*, 1511–1518.

(14) Mitragotri, S.; Johnson, M. E.; Blankschtein, D.; Langer, R. An analysis of the size selectivity of solute partitioning, diffusion, and permeation across lipid bilayers. *Biophys. J.* **1999**, *77*, 1268–1283.

(15) Xiang, T.-X.; Anderson, B. D. The relationship between permeant size and permeability in lipid bilayer membranes. *J. Membr. Biol.* **1994**, *140*, 111–121.

(16) Xiang, T.-X.; Anderson, B. D. Phospholipid surface density determines the partitioning and permeability of acetic acid in DMPC:cholesterol bilayers. *J. Membr. Biol.* **1995**, *148*, 157–167.

(17) Xiang, T.-X.; Anderson, B. D. Permeability of acetic acid across gel and liquid-crystalline lipid bilayers conforms to free-surface-area theory. *Biophys. J.* **1997**, *72*, 223–237.

(18) Xiang, T.-X.; Anderson, B. D. Phase structures of binary lipid bilayers as revealed by permeability of small molecules. *Biochim. Biophys. Acta* **1998**, *1370*, 64–76.

(19) Xiang, T.-X.; Anderson, B. D. Influence of chain ordering on the selectivity of dipalmitoylphosphatidylcholine bilayer membranes for permeant size and shape. *Biophys. J.* **1998**, *75*, 2658–2671.

(20) Xiang, T.-X.; Anderson, B. D. Influence of a transmembrane protein on the permeability of small molecules across lipid membranes. *J. Membr. Biol.* **2000**, *173*, 187–201.

(21) Xiang, T.-X.; Chen, J.; Anderson, B. D. A quantitative model for the dependence of solute permeability on peptide and cholesterol content in biomembranes. *J. Membr. Biol.* **2000**, *177*, 137–148.

(22) Hansch, C.; Leo, A. , *Substitutent Constants for Correlation Analysis in Chemistry and Biology*; Wiley-Interscience: New York, 1979.

(23) Rekker, R. F. *The Hydrophobic Fragmental Constant*; Elsevier: Amsterdam, 1977.

(24) Roseman, M. A. Hydrophilicity of polar amino acid side-chains is markedly reduced by flanking peptide bonds. *J. Mol. Biol.* **1988**, *200*, 513–522.

obtained from experimental transfer free energies of individual amino acids[25] or *N*-acetylamino acid amides or esters[26,27] have indicated that specific interactions such as intramolecular hydrogen bonding (i.e., "self-solvation") or other proximity effects involving flanking peptide bonds markedly reduce the hydrophilicity of polar amino acid side-chain residues.[24] More recently, hydrophobicity scales using data generated for blocked tripeptides[28,29] or pentapeptides[30] have been preferred as they are thought to better incorporate the interactions between adjacent residues in peptides, thereby enabling continued reliance on the framework provided by the structure-additivity assumption. Thus, the application of fragment-based LFERs to the estimation of peptide permeability may not require the absence of proximity or self-solvation effects, as long as these effects are approximately the same with varying peptide structure.

The significant role of proximity effects in peptide transfer processes was highlighted in the recent study by Mayer et al.,[9] who confirmed that the contribution of the peptide backbone -CONH- residue to the overall permeability is significantly reduced by flanking peptide residues. Specifically, their research determined the free energy contribution for the transfer of an isolated peptide amide residue from water to the hydrocarbon chain region of DOPC bilayers, $\Delta(\Delta G^\circ)_{\text{-CONH-}}$, to be 6.6 kcal/mol, whereas they reported a ~2 kcal/mol smaller value of $\Delta(\Delta G^\circ)_{\text{-CONH-}}$ for the same group in a series of peptides (4.6 kcal/mol), based on nonlinear regression analysis of permeabilities for a set of glycine-, alanine-, and sarcosine-containing peptides of *p*-toluic acid. The same study reported that, with increasing peptide length (from 1 to 3 residues), $\Delta(\Delta G^\circ)_x$ for the -Ala- or -Gly- residue contributions varied with peptide length and that the contribution of N-methylation (i.e., glycine→sarcosine) to the apparent transfer free energy varied significantly ($\Delta(\Delta G^\circ)_x = -0.5$ to -2.2 kcal/mol) with the position and number of *N*-methyl substituents in the permeant molecule. These latter observations suggested that proximity effects may be dependent on the specific nature of the flanking residue.

In this study, we consider the influence of the $i-1$ and $i+1$ residues flanking a given glycine (*i*th residue) in a series of mono-, di-, and tripeptides on the -Gly- residue contribution to the apparent free energy of peptide transfer from water to the hydrocarbon chain region of a DOPC bilayer as reflected in permeability measurements at 25 °C or to various organic solvents including 1,9-decadiene, 1-octanol, and CCl_4 as determined by partition coefficients at 25 °C. A series of glycine-containing compounds (RGZ) and their reference compounds (RZ) lacking glycine, in which R represents the N-terminus and Z the C-terminus, were synthesized. The R-substituents were acetyl (Ac), *p*-toluyl (Tol), 4-methylphenyl acetyl (MPA), and 4-carboxymethylphenyl acetyl (CMPA), and the Z-substituents were -OH, -OMe, -NHMe, and -NMe_2.

Data generated for the above compounds were then combined with previously published data for permeability coefficients of model compounds obtained in DOPC (or egg PC) bilayers as well as decadiene/water partition coefficients from this and other laboratories, providing a 47-compound data set from which we constructed a new fragment-based LFER built from formic acid as the reference permeant. The contributions of nonpolar residues to the overall transfer free energy of each compound were evaluated from their calculated accessible surface areas and a single solvation parameter as described by Eisenberg et al.[31] Individual "isolated" free energy contributions for various polar fragments, including that for the peptide backbone -CONH-, were generated. Changes in the "isolated" value for the peptide backbone with variation in the acyl residue at the N-terminus($i-1$) and in the adjacent C-terminal ($i+1$) residue were assessed and correction terms necessary to account for the proximity or self-solvation effects of the $i+1$ flanking residue on the peptide backbone group contribution were determined.

Experimental Section

Materials. 1,2-Dioleoyl-*sn*-glycero-3-phosphocholine (DOPC, >99% purity) and 1,2-dioleoyl-*sn*-glycero-3-phosphate (DOPA, >99% purity) used to make liposomes for transport experiments were purchased from Avanti Polar-Lipids, Inc. (Pelham, AL). Three solvents, 1,9-decadiene (98%), 1-octanol (>99%) from Aldrich (Milwaukee, WI), and CCl_4 (99.6%) from Spectrum (New Brunswick, NJ), were used in the partitioning experiments. The solvents used for the syntheses, ethyl acetate, *N*,*N*-dimethylformamide (DMF), and dichloromethane (CH_2Cl_2), were obtained from Fisher (Fair Lawn, NJ). Three chemicals for the syntheses, trifluoroacetic acid (TFA, 99%), acetic acid (99.8%), and acetic anhydride (>97%), were also purchased from Fisher. All other chemicals for the syntheses, *N*-*tert*-butoxycarbonylglycine (*t*-Boc-G-OH, 98%), 1-hydroxybenzotriazole (HOBt, 99%), 1,3-dicyclohexylcarbodiimide (DCC, 99%), methylamine in THF (2 M), dimethylamine in THF (2 M), *N*,*N*-diisopropylethyl-

(25) Yunger, L. M.; Cramer, R. D. Measurement and correlation of partition coefficients of polar amino acids. *Mol. Pharmacol.* **1981**, *20*, 602–608.
(26) Fauchere, J.-L.; Pliska, V. Hydrophobic parameters p of amino-acid side chains from the partitioning of N-acetyl-amino-acid amides. *Eur. J. Med. Chem. - Chim. Ther.* **1983**, *18*, 369–375.
(27) Nandi, P. K. Thermodynamic parameters of transfer of N-acetyl ethyl esters of different amino acids from organic solvents to water. *Int. J. Peptide Protein Res.* **1976**, *8*, 253–264.
(28) Jacobs, R. E.; White, S. H. The nature of the hydrophobic binding of small peptides at the bilayer interface: Implications for the insertion of transbilayer helices. *Biochemistry* **1989**, *28*, 3421–3437.
(29) Kim, A.; Szoka, J., F.C. Amino acid side-chain contributions to free energy of transfer of tripeptides from water to octanol. *Pharm. Res.* **1992**, *9*, 504–514.
(30) Wimley, W. C.; Creamer, T. P.; White, S. H. Solvation energies of amino acid side chains and backbone in a family of host-guest pentapeptides. *Biochemistry* **1996**, *35*, 5109–5124.
(31) Eisenberg, D.; Wesson, M.; Yamashita, M. Interpretation of protein folding and binding with atomic solvation parameters. *Chem. Scr.* **1989**, *29A*, 217–221.

amine (DIEA, 99%), isobutyl chloroformate (IBCF, 98%), glycine methyl ester hydrochloride (G-OMe.HCl, 99%), *p*-tolylacetic acid (pTAA, 99%), and 1,4-phenylenediacetic acid (PDAA, 97%), were obtained from Aldrich. The commercially available model permeants, *p*-tolylacetic acid methyl ester (MPA-OMe, 99%), *N*,*N*-dimethylacetamide (Ac-NMe_2, >99%), and methyl acetate (Ac-OMe, 99%), were also purchased from Aldrich. Any model permeants commercially unavailable were synthesized as described below.

Synthesis. *t*-Boc-G-NMe_2 (*tert*-Butyl[2-(dimethylamino)-2-oxoethyl] carbamate). *t*-Boc-G-NMe_2 was prepared by adding DCC (2.17 g, 10.5 mmol) to a 25 mL stirred solution of *t*-Boc-G-OH (1.75 g, 10 mmol) and HOBt (1.42 g, 10.5 mmol) in DMF at 0 °C. After 30 min, 2 M dimethylamine (15 mmol) in THF was added, and the reaction mixture was stirred at 0 °C for 1 and 16 h at rt. The crude product after solids removal and solvent evaporation was dissolved in saturated aq $NaHCO_3$ solution (10 mL) and purified by ethyl acetate extraction (3 × 20 mL), sequential washing with citric acid solution (0.5 M, 10 mL) and saturated NaCl (10 mL), and filtration through anhydrous $MgSO_4$. After solvent removal, the product was dried in vacuo (rt, overnight) to provide a white powder (1.5 g, 75% yield). The mass spectrum agreed with the anticipated structure (parent ion $m/z = 203$ ($M + H^+$, CI)).

G-NMe_2 (2-Amino-*N*,*N*-dimethylacetamide), TFA Salt. TFA (5 mL) was added to a CH_2Cl_2 (10 mL) solution of *t*-Boc-G-NMe_2 (1.5 g) and incubated for 2 h (rt). After solvent removal, the final product was crystallized (white needles, 1.3 g, 80% yield) from ethyl ether and dried in vacuo (rt, overnight). The mass spectrum of the product agreed with the anticipated structure (parent ion $m/z = 103$ ($M + H^+$, CI)).

G-NHMe (2-Amino-*N*-methylacetamide), TFA Salt. The same procedures as for G-NMe_2·TFA were employed but the nucleophile was 2 M methylamine in THF (7.5 mL, 15 mmol). The yields of *t*-Boc-G-NHMe and G-NHMe·TFA were 60% and 80%, respectively. The mass spectrum of the product agreed with the anticipated structure (parent ion $m/z = 89$ ($M + H^+$, CI)).

MPA-G-NMe_2 (*N*,*N*-Dimethylcarbamoylmethyl-2-*p*-tolylacetamide). IBCF (0.19 mL, 1.41 mmol) was added to a stirred solution of pTAA (0.27 g, 1.8 mmol) and DIEA (0.31 mL, 1.8 mmol) in 15 mL of DMF/CH_2Cl_2 (1:2) maintained at 0 °C under N_2. After 15 min, G-NMe_2·TFA (0.32 g, 1.5 mmol) and DIEA (0.26 mL, 2.0 mmol) in 1 mL ofDMF were added with stirring. After 45 min, the reaction mixture was diluted with water (3 mL), and the solvents were removed under N_2. The crude product was purified by HPLC (3:7 CH_3CN/pH 3 aq formic acid) and lyophilized to give a white powder (0.11 g, 0.47 mmol, 31%). The mass spectrum (parent ion $m/z = 235$ ($M + H^+$, CI)) and ^{1}H NMR ((200 MHz, $CDCl_3$) δ 2.34 (s, 3H, CH_3, *p*), 7.18 (s, 4H, *o, m*), 3.58 (s, 2H, -CH_2-), 4.01 (d, 2H, NCH_2), 2.96 (s, 6H, NCH_3)) agreed with the anticipated structure. Purity was >99% by HPLC.

Ac-G-NMe_2 (2-(Acetylamino)-*N*,*N*-dimethylacetamide). A procedure similar to that for MPA-G-NMe_2 (above) was employed with acetic acid replacing pTAA. The crude product was purified by HPLC (2:98 CH_3CN/pH 3 aq formic acid) and lyophilized to give a white powder (42% yield). The mass spectrum (parent ion $m/z = 167$ ($M + Na^+$, CI) and ^{1}H NMR ((200 MHz, D_2O) δ 2.067 (s, 3H, CH_3), 4.085 (s, 2H, $NHCH_2$), 3.050 (s, 3H, NCH_3), and 2.950 (s, 3H, NCH_3)) agreed with the anticipated structure. Purity was >99% by HPLC.

Ac-G-OMe (Methyl (Acetylamino)acetate). Acetic anhydride (0.57 mL, 6 mmol) was added to 10 mL of a sonicated (45 min) suspension of Na_2CO_3 (1.2 g, 11 mmol) and G-OMe·HCl (0.63 g, 5 mmol) in DMF, and the mixture was stirred at rt overnight. Following removal of solids, solvent was evaporated under N_2 and the crude product was purified by HPLC (2:98 CH_3CN/pH 3 formic acid solution) and lyophilized to give a white powder (0.122 g, 0.93 mmol, 19%). The mass spectrum (parent ion $m/z = 132$ ($M + H^+$, CI)) and ^{1}H NMR ((200 MHz, D_2O) δ 2.068 (s, 3H, CH_3), 4.01 (s, 2H, NCH_2), 3.77 (s, 3H, OCH_3)) agreed with the anticipated structure. Purity was >99% by HPLC.

MPA-NMe_2 (*N*,*N*-Dimethyl-2-*p*-tolylacetamide). IBCF (0.23 mL, 1.8 mmol) was added to a stirred solution of pTAA (0.23 g, 1.5 mmol) and DIEA (0.31 mL, 1.8 mmol) in 15 mL of DMF/CH_2Cl_2 (1:2) maintained at 0 °C under N_2. After 15 min, 2 M dimethylamine in THF (0.9 mL, 1.8 mmol) was added with stirring. After 45 min, the solvent was evaporated under a N_2 flow and the crude product was purified by HPLC (40:60 CH_3CN/pH 3 aq formic acid) and lyophilized leaving an oil (0.053 g, 0.3 mmol, 20%). The mass spectrum (parent ion $m/z = 200$ ($M + Na^+$, CI) and ^{1}H NMR ((200 MHz, D_2O) δ 2.33 (s, 3H, CH_3, *p*), 7.21 (d, 4H, o, m), 3.78 (s, 2H, CH_2), 3.03 (d, 6H, NCH_3)) agreed with the anticipated structure. Purity was >95% by HPLC.

MPA-NHMe (*N*-Methyl-2-*p*-tolylacetamide). IBCF (0.78 mL, 6 mmol) was added to a stirred solution of pTAA (0.75 g, 5 mmol) and DIEA (0.92 mL, 5 mmol) in 15 mL of DMF/THF (1:2) maintained at 0 °C under N_2. After 15 min, 2 M methylamine in THF (3.0 mL, 6 mmol) was added with stirring. After 45 min, under the same conditions the reaction mixture was diluted with water (3 mL) and solvents were evaporated under N_2. The residue was extracted into ethyl acetate (10 mL), and the organic phase was washed sequentially with saturated $NaHCO_3$ (20 mL), 0.5 M citric acid solution (10 mL), and saturated NaCl (10 mL). After solvent removal, the crude product was purified by HPLC (25:75 CH_3CN/pH 3 aq formic acid) and lyophilized to give a white powder (0.2 g, 1.2 mmol, 24%). The mass spectrum (parent ion $m/z = 164$ ($M + H^+$, CI)) and ^{1}H NMR ((200 MHz, $CDCl_3$) δ 2.36 (s, 3H, CH_3, *p*), 7.16 (s, 4H, *o, m*), 3.55 (s, 2H, CH_2), 2.76 (d, 3H, NCH_3)) agreed with the anticipated structure. Purity was >95% by HPLC.

MPA-G-NHMe (*N*-Methylcarbamoylmethyl-2-*p*-tolylacetamide). The synthetic procedure was the same as that for MPA-G-NMe_2. The reactants were pTAA (0.18 g, 1.2 mmol), DIEA (0.38 mL, 2.2 mmol), IBCF (0.16 mL, 1.2 mmol), and G-NHMe·TFA (0.19 g, 1 mmol). The crude product was purified by HPLC (25:75 CH_3CN/pH 3 aq formic acid) and lyophilized to yield a white powder (0.08

g, 0.36 mmol, 36%). The mass spectrum (parent ion m/z = 243 ($M + Na^+$, CI)) and ^1H NMR ((200 MHz, $CDCl_3$); δ 2.35 (s, 3H, CH_3, *p*), 7.17 (s, 4H, o, m), 3.58 (d, 2H, CH_2), 3.86 (d, 2H, NCH_2), 2.79 (d, 3H, NCH_3)) agreed with the anticipated structure. Purity was >99% by HPLC.

MPA-G-OMe (2-*p*-Tolylacetylamino)acetic Acid Methyl Ester. IBCF (0.26 mL, 2.0 mmol) was added to a solution of pTAA (0.30 g, 2.0 mmol) and DIEA (0.35 mL, 2.0 mmol) in 15 mL of DMF/THF (1:2) maintained at 0 °C under N_2. After 15 min, a mixture of G-OMe·HCl (0.30 g, 2.4 mmol) and DIEA (0.42 mL, 2.4 mmol) in DMF (2 mL) was added, and after 45 min under the same conditions, the reaction mixture was diluted with 10 mL of water and extracted into ethyl acetate (30 mL). The organic phase was washed sequentially (saturated $NaHCO_3$ (20 mL), 0.5 M citric acid solution (20 mL), and saturated NaCl (20 mL)), filtered (anhydrous $MgSO_4$), and evaporated to yield a white powder (0.19 g, 0.85 mmol, 43%). The mass spectrum (parent ion m/z = 244 ($M + Na^+$, CI)) and ^1H NMR ((200 MHz, $CDCl_3$) δ 2.35 (s, 3H, CH_3, p), 7.18 (s, 4H, o, m), 4.01 (d, 2H, NCH_2), 3.73 (s, 3H, OCH_3)) agreed with the anticipated structure. Purity was >99% by HPLC.

MPA-G-OH ({[(4-Methylphenyl)acetyl]amino}acetic Acid). IBCF (0.26 mL, 2.0 mmol) was added with stirring to pTAA (0.30 g, 2 mmol) and DIEA (0.34 mL, 2.0 mmol) in DMF (15 mL) maintained at 0 °C under N_2. After 15 min, glycine (0.30 g, 4 mmol) in a sufficient amount of 1.0 M NaOH to obtain a pH 10.1 solution was added, and after 45 min under the same conditions, the solvent was evaporated under N_2. The crude product was purified by HPLC (30:70 CH_3CN/pH 3 aq formic acid) and lyophilized to produce a white powder (0.074 g, 0.42 mmol, 20% yield). The mass spectrum (parent ion m/z = 230 ($M+Na^+$, CI)) and ^1H NMR ((200 MHz, $CDCl_3$) δ 2.36 (s, 3H, CH_3, *p*), 7.18 (s, 4H, *o, m*), 4.05 (d, 2H, NCH_2), 3.62 (s, 2H, CH_2)) agreed with the anticipated structure. Purity was >99% by HPLC.

CMPA-NMe_2 ({4-[2-(Dimethylamino)-2-oxoethyl]phenyl}acetic Acid). IBCF (0.34 mL, 2.6 mmol) was added with stirring to PDAA (0.5 g, 2.6 mmol) and DIEA (0.54 mL, 3.1 mmol) in DMF (20 mL) maintained at −10 °C (dry ice/acetone). After 10 min, 2 M dimethylamine in THF (1.0 mL, 2 mmol) was added, and the reaction mixture was stirred for 30 min (rt) under N_2. The solvent was evaporated under N_2, and the crude product was purified by HPLC (20:80 CH_3CN/pH 3 aq formic acid) and lyophilized to produce a white powder (0.10 g, 0.45 mmol, 23%). The mass spectrum (parent ion m/z = 222 ($M + H^+$, CI)) and ^1H NMR ((200 MHz, $CDCl_3$) δ 3.65 (s, 2H, -CH_2-, *p*), 7.25 (s, 4H, *o, m*), 3.72 (s, 2H, -CH_2-), 2.99 (d, 6H, NCH_3)) agreed with the anticipated structure. Purity was >99% by HPLC.

CMPA-G-NMe_2([4-(2-{[2-(Dimethylamino)-2-oxoethyl]-amino}-2-oxoethyl)phenyl]acetic Acid). DCC (0.64 g, 3 mmol) was added with stirring to PDAA (0.96 g, 5 mmol) and HOBt (0.5 g, 0.37 mmol) in DMF (30 mL) maintained at 0 °C. After 30 min, G-NMe_2·TFA (0.56 g, 2.6 mmol) and DIEA (0.55 mL, 3 mmol) in CH_2Cl_2 (5 mL) were added with stirring, and the reaction mixture was incubated 0 °C (1 h) and at rt for 16 h. After filtration to remove solid and solvent evaporation under N_2, the crude product was dissolved in 1 M NaOH to obtain a pH 8 solution and purified by HPLC using water as mobile phase. Lyophilization produced a white powder (0.13 g, 0.47 mmol, 18%) having a mass spectrum (parent ion m/z = 301 ($M + Na^+$)) and ^1H NMR ((200 MHz, $CDCl_3$); δ 3.54 (s, 2H, -CH_2-, *p*), 7.29 (s, 4H, *o, m*), 3.68 (s, 2H, -CH_2-), 4.07 (d, 2H, NCH_2), 2.98 (d, 6H, NCH_3) that were consistent with the anticipated structure. Purity was >99% by HPLC.

HPLC Conditions for the Purifications and Analyses. The HPLC system used in the study consisted of a Waters (Milford, MA) 515 HPLC pump, a Waters 717plus autosampler, a Waters 2487 dual λ absorbance detector and an SRI Instruments (Torrance, CA) Model 302 data system. The data were collected and analyzed by PeakSimple chromatography software (SRI Instruments version 3.29). The purifications of the compounds synthesized employed an analytical C18 column (Supelcosil, LC-ABZ+Plus; 25 cm × 4.0 mm i.d., Supelco, St. Louis, MO) and a 1 mL injection volume. The wavelength used in the purifications was 254 nm for products with a phenyl group and 220 nm for those lacking a phenyl group. The mobile phases used in the purifications were described in the synthesis section. Mobile phases used for the HPLC analyses contained CH_3CN and pH 3 formic acid solutions at ratios of 50:50 (v/v) for MPA-G-OH, MPA-OMe, and MPA-G-OMe; 40:60 (v/v) for MPA-NMe_2, MPA-G-NMe_2, and MPA-OH; 2:98 (v/v) for Ac-OMe, Ac-G-OMe, Ac-NMe_2, and Ac-G-NMe_2; 35:65 (v/v) for MPA-NHMe and MPA-G-NHMe; and 20:80 (v/v) for CMPA-G-NMe_2. The mobile phase for CMPA-NMe_2 was 20:80, v/v, CH_3CN/20 mM pH 3 $NH_4H_2PO_4$ solution. A wavelength of 220 nm was used for the analyses of all model compounds. The flow rate was 1 mL/min for the purifications and HPLC analyses.

pK_a Measurements. Ionization constants for CMPA-NMe_2 and CMPA-G-NMe_2 were determined at 25 °C using a microtitration technique.[32] A 150 μL aliquot of a 0.001 M solution of CMPA-NMe_2 was titrated with 0.1 M NaOH, while a 200 μL aliquot of a 0.002365 M solution of CMPA-G-NMe_2 was titrated with 0.1 M HCl. Plots of pH versus titrant volume were fit to ionic equilibria models to determine apparent pK_a values.

Bulk Solvent Partition Coefficients. 1,9-Decadiene/water partition coefficients (PC = C_{org}/C_{aq}) were determined for all RGZ/RZ compounds. CCl_4/water and 1-octanol/water partition coefficients were also obtained for some compounds. Before the experiments, the organic solvents were washed (3×) with equal portions of deionized water. Stock solutions of model compounds in deionized water or in 0.1 N HCl (for CMPA and MPA-G-OH series of compounds) were equilibrated with the organic solvent using the shake

(32) Morgan, M. E.; Liu, K.; Anderson, B. D. Microscale titrimetric and spectrophotometric methods for determination of ionization constants and partition coefficients of new drug candidates. *J. Pharm. Sci.* **1998**, *87*, 238–245.

flask method[33] at 25 °C. The overall concentration range for all model compounds was from 10^{-6} to 10^{-1} M. The lowest aqueous concentration for each compound was based on preliminary partitioning studies to ensure that the equilibrium concentrations in both aqueous and organic phases were higher than the limit of quantitation. Single determinations of the partition coefficient were performed at each of three concentrations which varied by ~4−100-fold. Aqueous solute concentrations were directly determined by HPLC, and those in the organic phases were either calculated from the changes in concentration in the corresponding aqueous phases before and after equilibrium or determined by back-extraction of solute from the organic phases followed by HPLC analyses.

Transport Experiments. Apparent DOPC bilayer permeability coefficients of CMPA-NMe_2 and CMPA-G-NMe_2 were obtained by monitoring solute efflux at 25 °C as described previously.[9,34] Solutions of DOPC/DOPA (96:4, molar ratio) in $CHCl_3$ were transferred to a set of glass tubes, where the $CHCl_3$ was removed under a N_2 flow to form a thin lipid film. The lipid film was suspended in a solution of the solute at a given pH followed by extrusion (17x) through a 0.2 μm membrane (Nuclepore Track-Etch Membrane, Whatman, Florham Park, NJ) to generate large unilamellar vesicles (LUV) containing permeant. The extravesicular solute was removed using a size exclusion column (PD-10 desalting column; GE Health Care (Amersham Biosciences); Piscataway, NJ) to create a concentration gradient. Solute efflux was determined as a function of time by ultrafiltration (Centricon YM-100; Millipore; Bedford, MA).

Apparent permeability coefficients (P_{app}) at each pH were calculated from the ultrafiltered permeant concentration vs time profiles by using eqs 1 and 2, in which C_0, C_t, and C_∞ are the initial extravesicular solute concentration, concentration at time t, and concentration when transport is complete; k_{obs} is the observed first order transport rate constant; and P_{app} is the apparent permeability coefficient.

$$C_t = C_\infty - (C_\infty - C_0)e^{-k_{obs}t} \quad (1)$$

$$P_{app} = k_{obs}d/6 \quad (2)$$

The pH dependence of the permeability coefficient enables one to calculate the intrinsic permeability coefficient (P_{HA}) of the un-ionized species by using eqs 3 and 4, in which f_{HA} is the fraction of un-ionized species and pK_a is the negative logarithm of the permeant ionization constant.

$$P_{app} = f_{HA}P_{HA} \quad (3)$$

$$f_{HA} = 1/(1 + 10^{pH-pKa}) \quad (4)$$

Calculation of Functional Group Contributions to the Free Energy of Solute Transfer. The value obtained for transfer free energy depends on the concentration scale (molarity, molality, or mole fraction) chosen in the calculations.[35,36] In the current study, the molarity concentration scale was used to calculate transfer free energies for both permeation and partitioning data.

The contribution of a given functional group or substituent, x, to the molar free energy of solute transfer from water to the organic solvent environment of interest at 25 °C, $\Delta(\Delta G°)_x$, was determined by comparing the intrinsic permeability coefficient (P) or partition coefficient (PC) of the substituted compound to that of a reference compound lacking the substituent. The general relationships are expressed in eqs 5 and 6, where "sub" stands for the substituted compound and "ref" for the reference compound.

$$\Delta(\Delta G^\circ)_x = -RT\ln(P_{sub}/P_{ref}) \quad (5)$$

$$\Delta(\Delta G^\circ)_x = -RT\ln(PC_{sub}/PC_{ref}) \quad (6)$$

Development of a Fragment-Based Linear Free Energy Relationship (LFER) for Lipid Bilayer Permeability. The fragment-based approach commonly employed in studies of transfer processes for peptides and proteins assumes that the polar and nonpolar portions of the peptide contribute additively to the overall solvation free energy.[4,30] The details for the construction of the LFER relationship developed herein are explained in two steps:

Model Compounds and Depiction of Fragments. In order to construct the LFER, data from this study and previous literature results for solute transfer from water to the hydrocarbon chain interior of DOPC (egg PC) bilayers (from permeability coefficients) or 1,9-decadiene, a solvent that resembles the barrier domain for lipid bilayer transport, [8,13] were combined, resulting in a 47-compound data set ranging in structural complexity from small monofunctional molecules to tripeptides. Formic acid was used as the reference compound. The general structures of all model compounds built from formic acid are depicted in Table 3, where W, R_1, R_2, and Y are substituent fragments.

Regression Analyses. For a typical process involving the transfer of a given model compound from water to decadiene or the barrier domain of a lipid bilayer, the overall transfer free energy can be expressed as a sum of the value for the reference compound (formic acid) plus the change in transfer free energy contributed by replacing portions of formic acid with new substituents to construct the model compound of interest:

$$\Delta G^\circ_{tot} = \Delta G^\circ_{HCOOH} + \Delta(\Delta G^\circ)_x \quad (7)$$

in which $\Delta G°_{tot}$ and $\Delta G°_{HCOOH}$ are the total transfer free energies of the model compound of interest and formic acid, respectively, and $\Delta(\Delta G°)_x$ reflects the combined change in transfer free energy contributed by all fragments removed

(33) Leo, A.; Hansch, C.; Elkins, D. Partition coefficients and their uses. *Chem. Rev.* **1971**, *71*, 525–616.

(34) Xiang, T.-X.; Xu, Y.-H.; Anderson, B. D. The barrier domain for solute permeation varies with lipid bilayer phase structure. *J. Membr. Biol.* **1998**, *165*, 77–90.

(35) Auton, M.; Bolen, D. W. Additive transfer free energies of the peptide backbone unit that are independent of the model compound and the choice of concentration scale. *Biochemistry* **2004**, *43* (5), 1329–42.

(36) Ben-Naim, A. Standard thermodynamics of transfer. Uses and misuses. *J. Phys. Chem.* **1978**, *82* (7), 792–803.

from and/or added to formic acid. Apparent values of $\Delta(\Delta G^\circ)_x$ can be obtained experimentally according to eq 5 and/or eq 6 by comparing the permeability and/or partition coefficient of the model compound to those of formic acid.

Typically, $\Delta(\Delta G^\circ)_x$ may consist of both nonpolar and polar contributions. The nonpolar contribution can be formulated as[9,26,30,31,37]

$$\Delta(\Delta G^\circ)_{np} = \sigma_{np}\Delta A_{np}$$

in which σ_{np} is the nonpolar solvation parameter and ΔA_{np} ($A_{np} - A_{np}$(formic acid)) is the change in overall solvent-accessible surface area for the nonpolar portion of any given compound (A_{np}) from that of formic acid (27.8 Å^2), which can be obtained from the sum of individual solvent-accessible surface areas of the constituent nonpolar residues

$$\sigma_{np}\Delta A_{np} = \sigma_{np}\sum_{i=1}^{m}\Delta A_{np,i}$$

In this study, A_{np} was obtained from molecular structures constructed using the xLeap algorithm in AMBER 8 (University of California, San Francisco, CA). The nonpolar surface area (A_{np}) excluding the polar functional groups was then calculated using VEGA ZZ software (http://www.d-dl.unimi.it) and a water molecule (1.4 Å radius) as a probe. The fast double cubic lattice model[38] incorporated into VEGA ZZ was used to estimate solvent-accessible surface area. While some polar functional groups contain both nonpolar and polar regions, the nonpolar surface area contributions from polar residues were not considered in summing the nonpolar surface area in this study. Values for ΔA_{np} were obtained from A_{np} by subtracting the nonpolar surface area of formic acid (27.8 Å^2).

The polar contribution of the corresponding compound, $\Delta(\Delta G^\circ)_p$, is a sum of the contributions from individual polar functional groups (e.g., -CON<, -O-, -Cl, etc.) minus the -COOH contribution in formic acid. Polar contributions for different types of individual hydrogen atoms attached to heteroatoms (i.e., -OH, -COOH, -CON*H*-, etc.) were considered separately. Consequently, $\Delta(\Delta G^\circ)_x$, with formic acid as a reference solute, is expressed in general form as

$$\Delta(\Delta G^\circ)_x = \sigma_{np}\sum_{i=1}^{m}\Delta A_{np,i} + \sum_{j=1}^{n}\Delta(\Delta G^\circ)_{p,j} \qquad (8)$$

in which the overall nonpolar and polar contributions are represented by the summation of the contributions of various fragments.

As noted in the Introduction, intramolecular hydrogen bonding or other proximity effects caused by flanking peptide residues are expected to alter the contribution of the peptide backbone -CON< residue compared to the value of an isolated -CON<. Therefore, a set of correction terms reflecting the C-terminal ($i + 1$) neighboring residue effect on the group contribution of the ith peptide bond were incorporated into eq 8 for $\Delta(\Delta G^\circ)_{\text{-CON<}}$. The resulting relationship is shown in eq 9:

$$\Delta(\Delta G^\circ)_x = \sigma_{np}\sum_{i=1}^{m}\Delta A_{np,i} + \sum_{j=1}^{n}\Delta(\Delta G^\circ)_{p,j} + \sum_{k=1}^{q}\Delta(\Delta G^\circ)_{corr,k} \qquad (9)$$

in which $\Delta(\Delta G^\circ)_{corr,k}$ represents correction terms for the four different types of $i + 1$ linkages examined (-OMe, -OH, -NH-, and -NMe-).

Equation 9, which is applicable to solute partitioning from water to decadiene, $\Delta(\Delta G^\circ)_x$ (PC), can be rearranged to the following equation:

$$\mathrm{PC} = 6.2\times10^{-4}\exp\left[-\left(\sigma_{np}\sum_{i=1}^{m}\Delta A_{np,i} + \sum_{j=1}^{n}\Delta(\Delta G^\circ)_{p,j} + \sum_{k=1}^{q}\Delta(\Delta G^\circ)_{corr,k}\right)/RT\right] \qquad (10)$$

in which 6.2×10^{-4} is the decadiene/water partition coefficient of formic acid.

While solute size effects on bulk solvent/water partition coefficients are relatively unimportant when they are based on the molar concentration scale,[35,36] permeability coefficients in lipid bilayers and other biological membranes can be highly sensitive to the size of the permeant.[11,15,19,39,40] Since formic acid, the reference compound in the above LFER model, is significantly smaller than most of the permeants evaluated, apparent transfer free energies derived from relative permeability coefficients across DOPC bilayers required a size correction before they could be combined with transfer free energies obtained from partition coefficients. Relationships previously developed in these laboratories for the dependence of the permeability coefficient across egg PC bilayers on permeant volume[15] suggested the following empirical equation for correcting permeability coefficients for permeant size

$$\ln\frac{P}{\mathrm{PC}} = \ln\frac{D_0}{\delta} - n\ln V$$

where P and PC are the permeability coefficient and partition coefficient of a permeant having molecular volume V; $\ln D_0/\delta$ is the intercept in the above equation (at $V = 1.0$ Å^3); and n is the size selectivity parameter. With appropriate rearrangement, the correction for the size of permeant can be transformed into a free energy contribution

(37) Eisenberg, D.; McLachlan, A. D. Solvation energy in protein folding and binding. *Nature* **1986**, *319*, 199–203.

(38) Eisenhaber, F.; Lijnzaad, P.; Argos, P.; Sander, C.; Scharf, M. The double cubic lattice method: efficient approaches to numerical integration of surface area and volume and to dot surface contouring of molecular assemblies. *J. Comput. Chem.* **1995**, *16* (3), 273–84.

(39) Anderson, B. D.; Raykar, P. V. Solute structure-permeability relationships in human stratum corneum. *J. Invest. Dermatol.* **1989**, *93*, 280–286.

(40) Stein, Nir. On the mass dependence of diffusion within biological membranes and polymers. *J. Membr. Biol.* **1971**, *5*, 246–249.

$$nRT\ln\frac{V_{sub}}{V_{ref}}$$

and substituted into eq 9 to get eq 11, which is applicable to changes in transfer free energy for molecular transport across lipid bilayers (not applicable to partition coefficients):

$$\Delta(\Delta G^{\circ})_x = nRT\ln\frac{V_{sub}}{V_{ref}} + \sigma_{np}\sum_{i=1}^{m}\Delta A_{np,i} + \sum_{j=1}^{n}\Delta(\Delta G^{\circ})_{p,j} + \sum_{k=1}^{q}\Delta(\Delta G^{\circ})_{corr,k} \quad (11)$$

where V_{sub} and V_{ref} are the molecular volumes of the substituted and reference compound (formic acid), respectively. Molecular volumes were estimated from the van der Waals increments of the individual atoms[41]

$$V = \sum_{i=1}^{M} V_i$$

where there are M atoms in a chemical structure, and each atom has a van der Waals increment of V_i. The molecular volume of each model compound is listed in Table 3. The following equation was used to predict permeability coefficients across DOPC bilayers at 25 °C

$$P = 2.9\times10^{-3}\exp\left[-\left(nRT\ln\frac{V_{sub}}{V_{ref}} + \sigma_{np}\sum_{i=1}^{m}\Delta A_{np,i} + \sum_{j=1}^{n}\Delta(\Delta G^{\circ})_{p,j} + \sum_{k=1}^{q}\Delta(\Delta G^{\circ})_{corr,k}\right)/RT\right] \quad (12)$$

in which 2.9×10^{-3} cm/s is the permeability coefficient for formic acid across the DOPC/eggPC bilayer at 25 °C.

Regression Analyses. Scientist (Micromath, St. Louis, MO) was used for all nonlinear least-squares regression analyses.

Results

Partition Coefficients for RGZ/RZ Compounds. Partition coefficients (PC) determined in this study for a series of RGZ/RZ pairs of compounds are listed in Table 1 for 1,9-decadiene/H_2O, CCl_4/H_2O, and 1-octanol/H_2O at 25 °C. The solute concentration in the aqueous phase at equilibrium was systematically varied, and the logarithms of partition coefficient for each compound were plotted against the logarithms of aqueous concentration at equilibrium in Figure 1. As shown in Figure 1, log PC is constant with increasing log C(aq), indicating the insensitivity of the partition coefficients to changes in solute concentration. These results provide evidence for the absence of significant self-association effects in all combinations of model compounds and solvents at the concentrations employed.

Passive Transport of CMPA-Peptides across DOPC Lipid Bilayers. Transport experiments were conducted for CMPA-G-NMe_2/CMPA-NMe_2 across DOPC bilayers (96:4 DOPC/DOPA molar ratio) at 25 °C. The presence of an ionizable -COOH in both members of this RGZ/RZ pair enabled reliable determination of permeability coefficients by adjusting the solution pH to a region where permeability was membrane-controlled rather than aqueous diffusion-controlled. The pK_a values of both CMPA-NMe_2 and CMPA-G-NMe_2 required in eq 4 were determined using the microscale titrimetric method,[32] yielding 4.37 ± 0.02 and 4.38 ± 0.05, respectively. A typical solute efflux profile (extravesicular concentration vs time) for CMPA-G-NMe_2 at pH 8.31 is depicted in Figure 2 (top panel). The line is the fit according to eq 1, from which a first order transport rate constant, k_{obs}, was calculated. P_{app} values at different pH were obtained by substituting k_{obs} into eq 2. The profiles of P_{app} vs pH, shown in the lower panel of Figure 2, were used to calculate the intrinsic permeability coefficients of the model compounds according to eqs 3 and 4.

Table 1. Organic Solvent/Water Partition Coefficients at 25 °C Generated in This Study for Various RGZ/RZ Compound Pairs To Determine $\Delta(\Delta G^{\circ})_{gly}$[a]

	partition coefficient ± SD		
compd	1,9-decadiene/H_2O	CCl_4/H_2O	1-octanol/H_2O
Ac-OMe	1.18 ± 0.05		
Ac-G-OMe	$(7.35 \pm 0.09) \times 10^{-4}$		
Ac-NMe_2	$(6.2 \pm 0.4) \times 10^{-3}$		
Ac-G-NMe_2	$(1.30 \pm 0.06) \times 10^{-4}$		
CMPA-G-NMe_2	$(3.7 \pm 0.4) \times 10^{-6}$		
MPA-OH	0.41 ± 0.03	$(6.3 \pm 0.6) \times 10^{-1}$	
MPA-G-OH	$(3.9 \pm 0.5) \times 10^{-4}$	$(1.0 \pm 0.1) \times 10^{-3}$	
MPA-OMe	397 ± 11	599 ± 46	167 ± 18
MPA-G-OMe	$(2.94 \pm 0.08) \times 10^{-1}$	2.12 ± 0.04	16.0 ± 0.2
MPA-NMe_2	2.27 ± 0.04	11.4 ± 0.6	31.6 ± 0.5
MPA-G-NMe_2	$(4.0 \pm 0.1) \times 10^{-2}$	$(5.1 \pm 0.9) \times 10^{-1}$	6.9 ± 0.3
MPA-NHMe	$(2.17 \pm 0.03) \times 10^{-1}$	1.10 ± 0.03	
MPA-G-NHMe	$(1.1 \pm 0.1) \times 10^{-3}$	$(6.7 \pm 0.1) \times 10^{-2}$	

[a] Ac = acetyl; MPA = methyl phenylacetyl; and CMPA = carboxymethyl phenylacetyl.

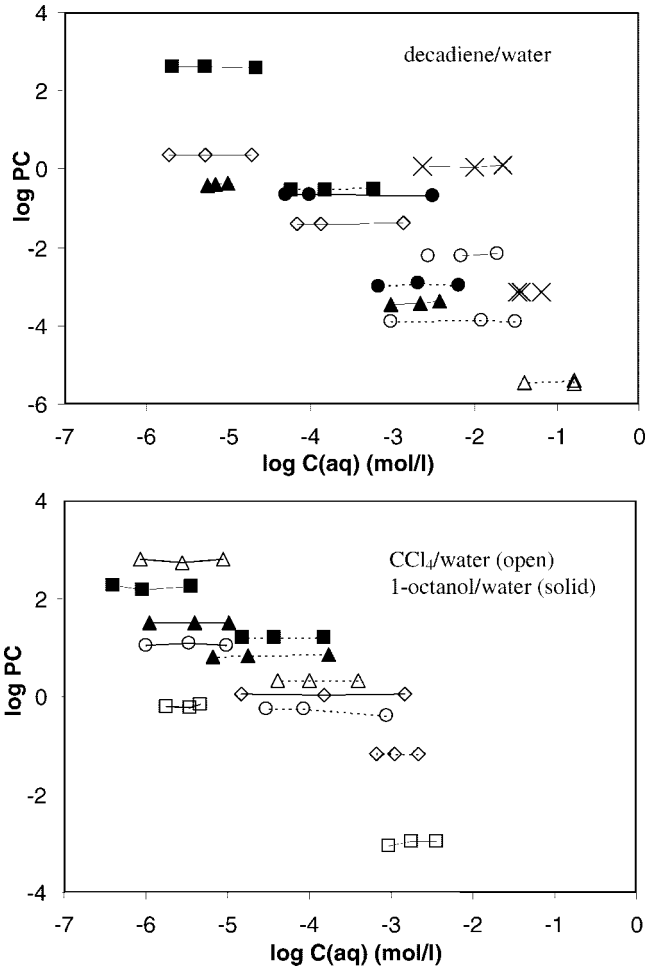

Figure 1. Plot of log PC vs log *C*(aq). *C*(aq) is the equilibrium concentration in the aqueous layer. In each panel, symbols with the same shape (either open or solid) represent compounds with the same R- and -Z. The dashed lines stand for compounds with glycine residues and solid lines are for compounds lacking glycine in decadiene [Upper panel (decadiene/water): X, (Ac, OMe);○, (Ac, NMe_2);▲, (MPA, OH);■, (MPA, OMe);◇, (MPA, NMe_2);•, (MPA, NHMe); Δ, (CMPA, NMe_2). Lower panel (CCl_4/water (open symbols)] and 1-octanol/water [(solid symbol): □: (MPA, OH);Δ: (MPA, OMe);○: (MPA, NMe_2);◇: (MPA, NHMe);■: (MPA, OMe);▲: (MPA, NMe_2)].

Determination of $\Delta(\Delta G^\circ)_{gly}$: Dependence on R-, -Z, and Solvent. The glycyl residue contribution to the transfer free energy from water into various organic solvents, $\Delta(\Delta G^\circ)_{gly}$, was calculated by comparing the partition coefficient of a glycine containing compound (RGZ) to that of its reference compound (RZ) using eq 6. Values of $\Delta(\Delta G^\circ)_{gly}$ for various RGZ/RZ pairs in different solvents are listed in Table 2.

Significant variability in the apparent $\Delta(\Delta G^\circ)_{gly}$ depending on the functional group (Z) at the C-terminus is evident in each solvent system, with a difference between the highest and lowest $\Delta(\Delta G^\circ)_{gly}$ of >2 kcal/mol generated from the decadiene/water partition coefficients. The values of

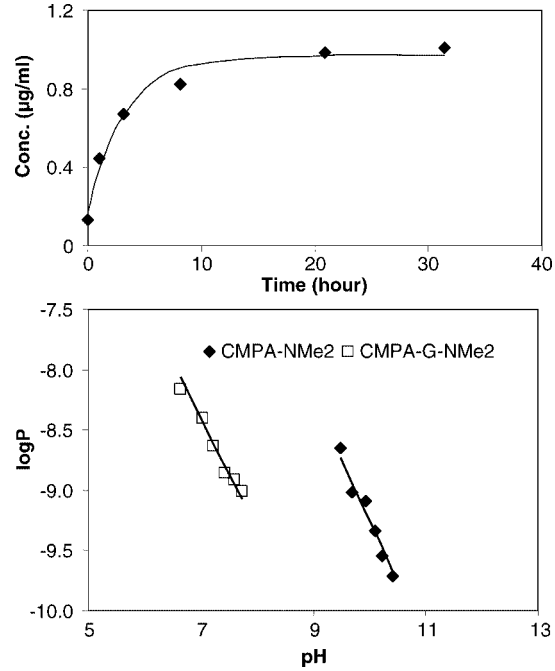

Figure 2. Upper panel: Plot of CMPA-G-NMe_2 extravesicular concentration vs time at pH 8.31. The solid line is the fit according to 1. Lower panel: log P_{app} vs pH profiles for CMPA-NMe_2 and CMPA-G-NMe_2. The lines are fits according to eqs 3 and 4.

$\Delta(\Delta G^\circ)_{gly}$ when Z = -NHMe (3.1 kcal/mol) or -NMe_2 (2.4 ± 0.1 kcal/mol) are consistently lower than the values of $\Delta(\Delta G^\circ)_{gly}$ when Z = -OH (4.4 ± 0.4) or -OMe (4.3 ± 0.1). The results also indicate that variations in the acyl substituent (R) at the N-terminus had no significant influence on $\Delta(\Delta G^\circ)_{gly}$ for a given C-terminus. This is also illustrated in Figure 3 where the observed R- and -Z dependence of the transfer free energy for a glycine residue, $\Delta(\Delta G^\circ)_{gly}$, is shown.

The compounds with R = MPA- were also studied in CCl_4/water, where again significant differences in the value of $\Delta(\Delta G^\circ)_{gly}$ are seen in comparing -O- containing with -N-containing -Z residues at the C-terminus. For each RGZ/RZ pair, $\Delta(\Delta G^\circ)_{gly}$ in CCl_4/water is lower than its counterpart in decadiene/water. Partition coefficients were determined in 1-octanol/water for two sets of compounds, MPA-G-NMe_2/MPA-NMe_2 and MPA-G-OMe/MPA-OMe. A third set was available in the literature. Although the values of $\Delta(\Delta G^\circ)_{gly}$ are further reduced in this compared to the other solvent systems, $\Delta(\Delta G^\circ)_{gly}$ remains significantly larger when Z = -OMe than when Z = -NMe_2 or -NHMe. These trends are more clearly seen in Figure 4, where $\Delta(\Delta G^\circ)_{gly}$ for the transfer of a glycine residue from water to three organic solvents is shown as a function of -Z.

LFER Analyses. Shown in Table 3 are the structures for the entire 47 compound data set along with partitioning and permeability data and apparent transfer free energies ($\Delta(\Delta G^\circ)_x$) for each compound relative to the reference compound, formic acid, calculated by comparing permeability or partition coefficients of the compound to that of formic acid according to eqs 5 or 6.

Table 2. $\Delta(\Delta G^\circ)_{gly}$ Determined from Various RGZ/RZ Pairs According to Eqs *5* and *6* Using Partition Coefficients (PC) in Various Solvents and Permeability Coefficients (*P*) across Egg PC or DOPC Bilayers[a,b]

		$\Delta(\Delta G^\circ)_{gly} \pm$ SD (cal/mol)			
R-	-Z	1,9-decadiene/H_2O (PC)	CCl_4/H_2O (PC)	1-octanol/H_2O (PC)	lipid bilayer (P)
MPA-	-OH	4102 ± 85	3806 ± 96		
Tol-	-OH	4654 ± 209[c]			4410 ± 80[c]
MPA-	-OMe	4257 ± 23	3305 ± 85	1389 ± 66	
Ac-	-OMe	4358 ± 25			
MPA-	-NMe_2	2385 ± 18	1845 ± 104	903 ± 27	
Ac-	-NMe_2	2288 ± 53			
CMPA-	-NMe_2	2493 ± 84			2773 ± 64
Tol-	-Sar-OH	2587[c]			2449[c]
Tol-	-Sar-G-OH	2487[c]			
MPA-	-NHMe	3105 ± 53	1662 ± 19		
Ac-	-NHMe			700[d]	
Tol-	-G-Sar-OH				3530[c]
Tol-Sar	-G-OH				3216[c]
Tol-	-G-OH				4400[c]
Tol-	-G-G-OH				3263[c]

[a] Ac = acetyl; MPA = methylphenylacetyl; CMPA = carboxymethyl phenylacetyl; Tol = *p*-toluyl; Sar = sarcosyl (−N(Me)CH_2CO−)). [b] Unless otherwise noted, data are from this study. [c] Data from Mayer et al.[9] [d] Data from Hansch et al.[22,72]

Figure 5 illustrates the nonpolar (blue dots) and polar (green dots) surface areas of Ac-G-NMe_2 as generated by VEGA ZZ software after energy minimization. The A_{np} values and molecular volumes calculated for each compound are also listed in Table 3. To compare surface areas generated in this study to previous results using other methods, average values of A_{np} were determined for the following nonpolar fragments: the methylene group (-CH_2-) inserted into an alkyl chain (from a comparison of surface areas of propionic, butyric, and hexanoic acids to that of the preceding homologue); the methylene group in a glycine residue (from a comparison of surface areas of glycine-containing solutes to their counterparts lacking the glycine residue of interest); and the backbone alkyl group in alanine (-$CH(CH_3)$-) following the same procedure as that described for the glycine methylene. The values (A_{np}) obtained were 35 ± 4, 39 ± 4, and 73 ± 0.3 Å^2, respectively, for the -CH_2- in an alkyl chain, the backbone -CH_2- in a glycine residue, and the alkyl group in alanine, respectively.

Partition coefficient-based $\Delta(\Delta G^\circ)_x$ values were substituted into eq 9, permeability coefficient-based values of $\Delta(\Delta G^\circ)_x$ were substituted into eq 11, and nonlinear regression analyses were performed to obtain group contributions for all polar groups along with the flanking C-terminal residue corrections to be applied to the backbone amide contribution. Estimates of σ_{np} for the contribution of nonpolar surface area to the free energy of transfer and the size selectivity parameter, *n*, applicable to DOPC or egg PC bilayer transport were also generated. The calculated values are listed in Table 4. (A sample calculation using the equations and values in Table 4 is provided in the Discussion.)

The calculated values of $\Delta(\Delta G^\circ)_x$ are plotted against their experimental counterparts, $\Delta(\Delta G^\circ)_x$ exptl in Figure 6. The slope is 0.993 and the coefficient of determination (0.993) suggests that >99% of the variance can be accounted for by the models described in eqs 9 and 11. Shown in Figure 7 are the results of a "leave one out" analysis of the data set in which each partition coefficient (top panel) or permeability coefficient (lower panel) for which experimental data were available was predicted from a regression analysis of the remaining data with the compound of interest omitted from the data set. The solid lines in these plots are the lines of identity (slopes = 1.0). Based on the coefficients of determination for the predicted versus observed values (i.e., 0.988 and 0.980), 98.8% and 98% of the variation in the permeability coefficients and partition coefficients, respectively, could be accounted for by the models employed. Another cross-validation was performed in which successive sets of data for 12 compounds representing 25% of the total data set were omitted. Compounds were grouped according to increasing complexity for this analysis. Coefficients of determination for the predicted versus observed values of the permeability coefficients and partition coefficients (data not shown) were 0.973 and 0.975, respectively.

Discussion

On the Validity of the Assumption of Independence and Additivity for the -CON< Group in Peptides. In a previous examination of the lipid bilayer permeabilities of a series of glycine, alanine, and sarcosine (Sar)-containing peptides of *p*-toluic acid (TOL-G_n, TOL-A_n, and TOL-Sar_m-G_n-Sar_l) where $n = 0-3$, $m = 0-2$, and $l = 0-2$ across egg PC bilayers at 25 °C,[9] several observations suggested that linear free energy relationships for predicting lipid bilayer transport of peptides may have limited utility due to apparent nonadditivities in residue group contributions. The following observations were indicative of nonadditivity in residue contributions: (1) the apparent backbone -CONH- residue contribution in peptides obtained from regression analysis of permeability coefficients was 4.6 kcal/mol, substantially

Table 3. Permeability (P) and Partition (PC) Coefficients[a] of the Compound Set Employed for LFER Development[h]

General Structure				Permeability Data		Partitioning Data		Solute Descriptors	
W-	-R_1-	-R_2-	-Y	P ± S.D. (cm/s)	$\Delta(\Delta G^\circ)_x$ (cal/mol)	PC ± S.D.	$\Delta(\Delta G^\circ)_x$ (cal/mol)	A_{pp} (Å^2)	V (Å^3)
Formic Acid									
H-			-OH	$(2.9 \pm 0.1) \times 10^{-3}$ [b]	-	$(6.2 \pm 0.4) \times 10^{-4}$ [b]	-	27.8	38.5
Alkanoic/benzoic acids and derivatives									
H-	-CH_2-		-OH	$(5.0 \pm 0.2) \times 10^{-3}$ [b]	-323	$(1.3 \pm 0.2) \times 10^{-3}$ [b]	-438	87.1	55.5
H-	-CH_2-		-NMe_2			$(6.2 \pm 0.5) \times 10^{-3}$	-1367	211	94.7
H-	-CH_2-		-OMe			1.18 ± 0.05	-4470	173.7	71
H-	-CH_2-	G	-NMe_2			$(1.30 \pm 0.06) \times 10^{-4}$	927	249.4	143.5
H-	-CH_2-	G	-OMe			$(7.35 \pm 0.09) \times 10^{-4}$	-101	214.1	119.8
H-	-$(CH_2)_2$-		-OH	$(2.6 \pm 0.1) \times 10^{-2}$ [c]	-1299			126.6	72.5
H-	-$(CH_2)_3$-		-OH	$(9.5 \pm 0.5) \times 10^{-2}$ [c]	-2066			159.4	89.5
H-	-$(CH_2)_5$-		-OH	1.1 ± 0.2 [c]	-3516			222.9	123.5
H-	-C_6H_4-		-OH	$(5.5 \pm 0.2) \times 10^{-1}$ [c]	-3106			184.4	107.9
p-Toluic acid series[d]									
H-	-CH_2-C_6H_4-		-OH	1.1 ± 0.2	-3516	0.90 ± 0.02	-4311	213.7	125.3
Cl-	-CH_2-C_6H_4-		-OH	$(6.4 \pm 0.1) \times 10^{-1}$	-3196	$(5.3 \pm 2.4) \times 10^{-1}$	-3997	172.1	139.4
CH_3-O-	-CH_2-C_6H_4-		-OH	$(3.5 \pm 0.1) \times 10^{-1}$	-2838	$(1.1 \pm 0.1) \times 10^{-1}$	-3066	249.4	148.5
CN-	-CH_2-C_6H_4-		-OH	$(2.7 \pm 0.5) \times 10^{-2}$	-1321	$(1.7 \pm 0.1) \times 10^{-2}$	-1961	172.5	144
HO-	-CH_2-C_6H_4-		-OH	$(1.6 \pm 0.4) \times 10^{-3}$	352	$(7.3 \pm 0.7) \times 10^{-4}$	-97	176.9	133
HOOC-	-CH_2-C_6H_4-		-OH	$(1.8 \pm 0.3) \times 10^{-4}$	1646	$(1.2 \pm 0.2) \times 10^{-4}$	972	167.1	152.4
H_2NOC-	-CH_2-C_6H_4-		-OH	$(4.1 \pm 0.4) \times 10^{-5}$	2522	$(4.0 \pm 0.7) \times 10^{-5}$	1623	162.2	156.6
p-Methylhippuric acid series[e]									
H-	-CH_2-C_6H_4-	G	-OH	$(4.9 \pm 0.4) \times 10^{-4}$	1053	3.4×10^{-4}	356	248.5	174.1
Cl-	-CH_2-C_6H_4-	G	-OH	$(3.5 \pm 0.5) \times 10^{-4}$	1252	2.0×10^{-4}	670	208.2	188.2
CH_3-O-	-CH_2-C_6H_4-	G	-OH	$(1.0 \pm 0.1) \times 10^{-4}$	1994	4.2×10^{-5}	1594	284.8	197.3
CN-	-CH_2-C_6H_4-	G	-OH	$(9.2 \pm 1.0) \times 10^{-6}$	3407	6.4×10^{-6}	2708	209.6	192.8
HO-	-CH_2-C_6H_4-	G	-OH	$(5.5 \pm 0.4) \times 10^{-7}$	5075	2.8×10^{-7}	4561	211.7	181.8
HOOC-	-CH_2-C_6H_4-	G	-OH	$(1.7 \pm 0.4) \times 10^{-7}$	5770	4.5×10^{-8}	5643	200.7	201.2
H_2NOC-	-CH_2-C_6H_4-	G	-OH	$(9.9 \pm 0.6) \times 10^{-9}$	7453	1.5×10^{-8}	6294	196.2	205.4
Tol- series[f]									
H-	-CH_2-C_6H_4-	G	-OH	$(6.4 \pm 0.5) \times 10^{-4}$	895	$(3.4 \pm 1.2) \times 10^{-4}$	356	248.5	174.1
H-	-CH_2-C_6H_4-	G-G	-OH	$(4.2 \pm 0.5) \times 10^{-7}$	5234			287.8	211.5
H-	-CH_2-C_6H_4-	G-G-G	-OH	$(1.7 \pm 0.3) \times 10^{-9}$	8497			325.4	254.6
H-	-CH_2-C_6H_4-	A	-OH	$(2.3 \pm 0.2) \times 10^{-3}$	137	$(2.2 \pm 0.1) \times 10^{-3}$	-750	286.7	191.1
H-	-CH_2-C_6H_4-	AA	-OH	$(1.1 \pm 0.1) \times 10^{-5}$	3301	$(1.1 \pm 0.3) \times 10^{-5}$	2387	360.2	256.9
H-	-CH_2-C_6H_4-	AAA	-OH	$(9.5 \pm 0.8) \times 10^{-8}$	6114			433.2	322.7
H-	-CH_2-C_6H_4-	Sar	-OH	$(1.5 \pm 0.1) \times 10^{-3}$	390	$(1.0 \pm 0.2) \times 10^{-3}$	-283	271.7	191.6
H-	-CH_2-C_6H_4-	Sar-G	-OH	$(3.2 \pm 0.3) \times 10^{-6}$	4032			308.7	240.4
H-	-CH_2-C_6H_4-	G-Sar	-OH	$(1.9 \pm 0.1) \times 10^{-5}$	2977	$(1.6 \pm 0.3) \times 10^{-5}$	2165	321.2	240.4
H-	-CH_2-C_6H_4-	Sar-G-G	-OH	$(1.4 \pm 0.1) \times 10^{-8}$	7248			345	289.2
H-	-CH_2-C_6H_4-	G-Sar-G	-OH	$(4.8 \pm 0.4) \times 10^{-8}$	6519			362.5	289.2
H-	-CH_2-C_6H_4-	G-G-Sar	-OH	$(4.9 \pm 0.1) \times 10^{-8}$	6507			363.1	289.2
H-	-CH_2-C_6H_4-	Sar-Sar-G	-OH	$(7.6 \pm 0.6) \times 10^{-8}$	6247			375.3	306.7
MPA- series[g]									
H-	-CH_2-C_6H_4-CH_2-		-OH	0.71 ± 0.07	-3257	0.40 ± 0.03	-3831	242.3	142.3
H-	-CH_2-C_6H_4-CH_2-		-NHMe			$(2.17 \pm 0.03) \times 10^{-2}$	-3469	323.1	164
H-	-CH_2-C_6H_4-CH_2-		-NMe_2			2.27 ± 0.04	-4859	356.2	181.5
H-	-CH_2-C_6H_4-CH_2-		-OMe			397 ± 11	-7917	328.1	162.3
H-	-CH_2-C_6H_4-CH_2-	G	-OH			$(3.9 \pm 0.5) \times 10^{-4}$	282	278.7	191.1
H-	-CH_2-C_6H_4-CH_2-	G	-NHMe			$(1.1 \pm 0.1) \times 10^{-3}$	-355	360.7	212.8
H-	-CH_2-C_6H_4-CH_2-	G	-NMe_2			$(4.0 \pm 0.1) \times 10^{-2}$	-2467	404.3	230.3
H-	-CH_2-C_6H_4-CH_2-	G	-OMe			0.294 ± 0.008	-3648	364.6	206.6
CMPA- series[g]									
HOOC-	-CH_2-C_6H_4-CH_2-		-NHMe	$(3.4 \pm 0.3) \times 10^{-5}$	2633	2.6×10^{-5}	1878	280.4	191.1
HOOC-	-CH_2-C_6H_4-CH_2-		-NMe_2	$(3.3 \pm 0.2) \times 10^{-4}$	1287	$(2.5 \pm 0.2) \times 10^{-4}$	538	318.1	208.6
HOOC-	-CH_2-C_6H_4-CH_2-	G	-NMe_2	$(1.6 \pm 0.3) \times 10^{-6}$	4461	$(3.7 \pm 0.4) \times 10^{-6}$	3038	363.7	257.4

[a] Data from this study unless otherwise noted. [b] From Xiang et al.[15] [c] From Walter et al.[43] [d] From Xiang et al.[13] [e] From ref 7. [f] From ref 8. [g] From ref 9. [h] Changes in apparent transfer free energy relative to formic acid ($\Delta(\Delta G^\circ)_x$) were derived from permeability (P) or partitioning (PC) data according to eqs 5 and 6. Nonpolar surface areas and molecular volumes are also listed.

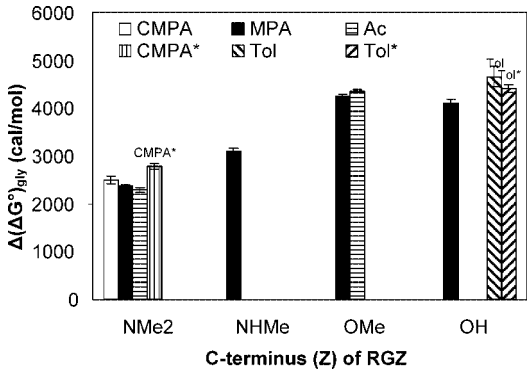

Figure 3. Observed R- and -Z dependence of the transfer free energy for a glycine residue, $\Delta(\Delta G^\circ)_{gly}$. $\Delta(\Delta G^\circ)_{gly}$ is independent of variations in R- (N-terminus). Partition coefficients (1,9-decadiene/water) used in the calculations of $\Delta(\Delta G^\circ)_{gly}$ are from Table 2, where *Z* = -NMe_2, -NHMe, -OMe or -OH. CMPA* and Tol* are calculated from permeability coefficients.

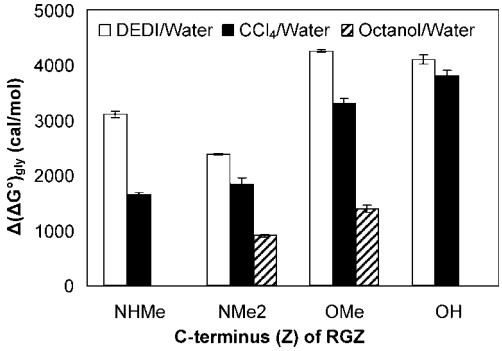

Figure 4. Free energy of transferring a glycine residue (RGZ/RZ series of compounds, where R = MPA and -Z = -NHMe, -NMe_2, -OMe, and -OH), $\Delta(\Delta G^\circ)_{gly}$, from water to three organic solvents. The apparent $\Delta(\Delta G^\circ)_{gly}$ depends on the variations in -Z and decreases with organic solvent polarizability and hydrogen-bonding capacity.

lower than the value estimated for an isolated -CONH- group of >6 kcal/mol; (2) the apparent glycine or alanine group contribution in Tol-G→Tol-GG→Tol-GGG or in Tol-A→Tol-AA→Tol-AAA decreased with increasing peptide length; and (3) the contribution of N-methylation was highly variable, depending on both the position of N-methylation and the number of N-methyl groups already on the molecule. Although a linear free energy relationship was identified that could adequately fit the peptide permeability data (12 compounds), it could not account for the above observations which were attributed to possible effects of intramolecular hydrogen bonding resulting in the formation of folded conformations, particularly in the nonpolar hydrocarbon region (i.e., barrier domain) of bilayers.

To confirm the reduced contribution of the backbone -CON< residue to the free energy of transfer from water to a hydrocarbon solvent or the barrier domain of liquid crystalline lipid bilayers compared to an isolated amide residue and to further explore the combined questions of independence and additivity of this contribution, we synthesized the series of RGZ/RZ compounds listed in Table 1 and determined their partition coefficients in several organic solvent/water systems and/or permeability coefficients in DOPC bilayers. Of particular interest was the sensitivity of the apparent contribution of a glycine residue to the free energies for these transfer processes with changes in R (the adjacent ($i - 1$) residue at the N-terminus) or Z (the adjacent ($i + 1$) residue on the C-terminus). The R- groups evaluated were toluyl, acetyl, 4-methylphenyl acetyl, and 4-carboxymethylphenyl acetyl, and the Z residues examined were -OH, -OMe, -NHMe, or -NMe_2.

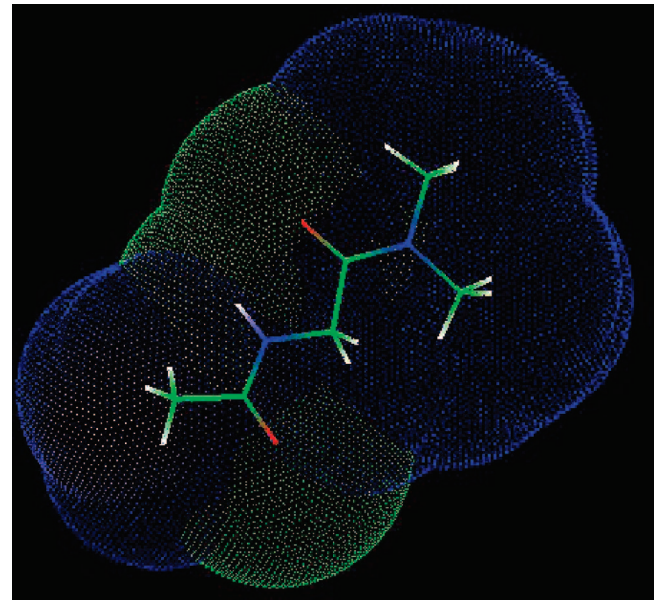

Figure 5. Illustration of the nonpolar (blue dots) and polar (green dots) surface areas of Ac-G-NMe_2 as generated by VEGA ZZ software. The structure was energy minimized in vacuum using a water molecule (r = 1.4 Å) as a probe of surface area.

Roseman[42] estimated the free energy of transfer of an "isolated" peptide bond $\Delta(\Delta G^\circ)_{\text{-CONH-}}$ from water into a nonpolar solvent environment to be 6.12 kcal/mol from the CCl_4/water partition coefficient of *N*-methylacetamide corrected by fragmental constants for the N-CH_3 and α-CH_3 groups. However, CCl_4 is inferior to a long chain hydrocarbon with some degree of unsaturation such as 1,9-decadiene[8,13] in terms of its ability to mimic the chemical selectivity of the barrier domain of liquid crystalline egg PC or DOPC bilayers. Thus, estimates of $\Delta(\Delta G^\circ)_{\text{-CONH-}}$ obtained from decadiene/water partition coefficients or bilayer permeability data are of interest. Previous results for carbamoyl (-$CONH_2$) substituted analogues of toluic or p-methylhippuric acid in these more relevant permeability or partitioning experiments gave $\Delta(\Delta G^\circ)_{\text{-CONH-}}$ of 6.1 and 6.4 kcal/mol, respectively.[7,13] Another estimate calculated for an isolated -$CONHCH_3$ substituted on the *p*-methyl position of tolylacetic acid[9]

(41) Edward, J. T. Molecular volumes and the Stokes-Einstein equation. *J. Chem. Educ.* **1970**, *47*, 261–270.

(42) Roseman, M. A. Hydrophobicity of the peptide *C*═O---H-N hydrogen-bonded group. *J. Mol. Biol.* **1988**, *201*, 621–623.

Table 4. Polar Functional Group Contributions to the Free Energy of Transfer from Water to 1,9-Decadiene or the Barrier Domain of DOPC or Egg PC Lipid Bilayers (Left Column) along with Neighboring Residue Corrections for the Peptide Backbone and Other Parameters Derived from Regression Analysis of the Data Set in Table *3* According to Eqs 9 and 11[a]

polar fragment	$\Delta(\Delta G^\circ)_p \pm$ SD (cal/mol)	adjacent C-terminal ($i+1$) residue	$\Delta(\Delta G^\circ)_{corr} \pm$ SD (cal/mol)
-COO-	2701 ± 239	-COOH or -COOMe	−1780 ± 154
-H (in -COOH)	1472 ± 189	-CONH- (-CONHMe)	−2656 ± 178
-CON<	6568 ± 202	-CONMe- (-CONMe$_2$)	−3365 ± 232
-H (first -CONH-)	357 ± 131	σ_{np} (cal/mol/ Å^2) (transfer from $H_2O \rightarrow$)	
-H (second -CONH$_2$)	−2201 ± 238	bilayer interior or 1,9 decadiene (this work)	−21.2 ± 0.5
-O- (ether or -OH)	1546 ± 185	bilayer interface	−13.1 ± 0.6[b]
-H (-OH)	1533 ± 235	1-octanol	−22.8 ± 0.8[c]
-Cl	−809 ± 174		−20.9 ± 2.5[d]
-CN	1228 ± 175	size selectivity parameter	
		n	0.84 ± 0.10

[a] The partition coefficient of a given compound can be calculated by:

$$\mathrm{PC} = 6.2\times10^{-4}\exp\left[-\left(\sigma_{np}\sum_{i=1}^{m}\Delta A_{np,i}+\sum_{j=1}^{n}\Delta(\Delta G^\circ)_{p,j}+\sum_{k=1}^{q}\Delta(\Delta G^\circ)_{corr,k}\right)/RT\right]$$

The permeability coefficient (cm/s, DOPC/egg PC bilayers) can be calculated by:

$$P = 2.9\times10^{-3}\exp\left[-\left(nRT\ln\frac{V_{sub}}{V_{ref}}+\sigma_{np}\sum_{i=1}^{m}\Delta A_{np,i}+\sum_{j=1}^{n}\Delta(\Delta G^\circ)_{p,j}+\sum_{k=1}^{q}\Delta(\Delta G^\circ)_{corr,k}\right)/RT\right]$$

[b] AcWL-X-LL transfer.[51] [c] AcWLm ($m = 1-6$).[30] [d] Ac-X amide transfer.[30]

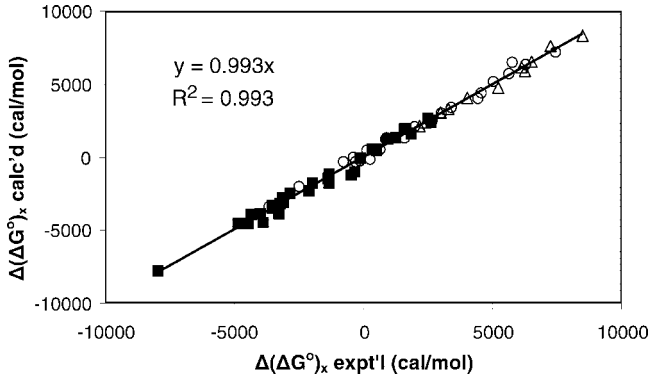

Figure 6. Plot of the calculated vs experimental $\Delta(\Delta G^\circ)_x$. $\Delta(\Delta G^\circ)_x$ (calcd) was obtained by fitting the data listed in Table 3 to eqs 9 and 11. Key: ■, compounds without amino acid residues; ○, compounds with one amino acid residue; and Δ, compounds with multiple amino acid residues.

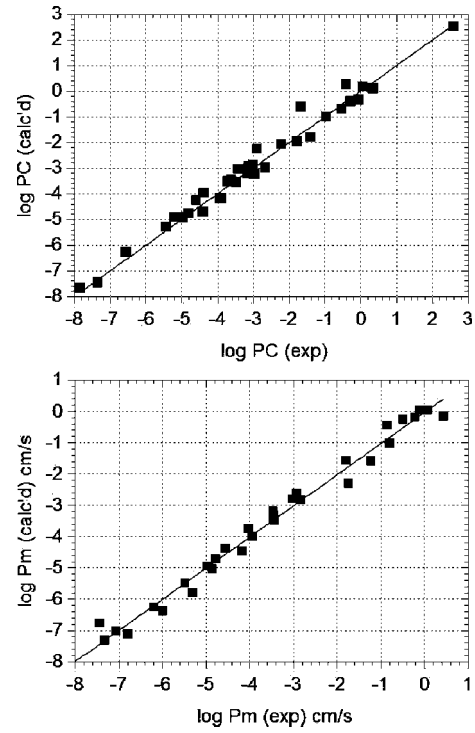

Figure 7. Plots of predicted log(PC) (upper panel) or log(*P*m) (lower panel) from the "leave one out" cross-validation analyses vs the corresponding experimental values. The solid lines are the lines of identity (slope = 1.0).

($\Delta(\Delta G^\circ)_{\text{-CONHCH2-}} = 5.8$ kcal/mol) gave a value for $\Delta(\Delta G^\circ)_{\text{-CONH-}}$ of 6.6 kcal/mol when adjusted for the normal methylene group contribution reported for lipid bilayer transport across egg PC (i.e., −764 cal/mol[43]). Thus, the value for $\Delta(\Delta G^\circ)_{\text{-CONH-}}$ appears to be >6 kcal/mol when the -CONH- group is well isolated from other polar substituents.

As revealed in the results in Table 2, the value of $\Delta(\Delta G^\circ)_{gly}$ derived from the RGZ/RZ series of compounds varies from 2.3−4.7 kcal/mol in decadiene/water and 1.7−3.8 kcal/mol in CCl_4/water, substantially smaller than the value of ∼5.8 kcal/mol obtained by combining the contributions of an isolated -CONH- and a methylene group. In examining the octanol/water partitioning data of Fauchère and Pliska[26] for *N*-acetylamino acid amides, Roseman previously noticed that proximity of the neighboring amide bond reduced the hydrophilicity of the -CONH- residue by 36%.[24] In the

(43) Walter, A.; Gutknecht, J. Monocarboxylic acid permeation through lipid bilayer membranes. *J. Membr. Biol.* **1984**, *77*, 255–264.

alkane/water system he estimated a reduction in $\Delta(\Delta G^\circ)_{\text{CONH-}}$ of nearly 3 kcal/mol, a value that appears to fall within the range illustrated in Table 2. Our results confirm that, regardless of the mechanism by which proximity or self-solvation effects occur, they must be taken into account in predicting peptide transport.

Considerable variability in $\Delta(\Delta G^\circ)_{\text{gly}}$ is evident within each column in Table 2, indicating a dependence on the neighboring substituents. To explore the source of the variability, the compounds in Table 2 were grouped according to their C-terminal residues (-Z). The results, plotted in Figure 4, confirm that the variability correlates with changes in -Z while $\Delta(\Delta G^\circ)_{\text{gly}}$ is insensitive to the changes in R- that were examined. The most significant differences in $\Delta(\Delta G^\circ)_{\text{gly}}$ occur when the values for -Z = -OH or -OMe (4.4 and 4.3 kcal/mol, respectively) are compared with those when -Z = -NHMe or $-NMe_2$ (3.1 and 2.4 kcal/mol, respectively). While the difference in $\Delta(\Delta G^\circ)_{\text{gly}}$ between the peptides with -O- vs -N-containing -Z residues was significant, there was not a significant difference when -Z = -OH vs -OMe. We were also unable to show a significant difference when -Z = -NHMe vs $-NMe_2$, due to the limited number of compounds compared.

The striking differences in $\Delta(\Delta G^\circ)_{\text{gly}}$ depending on the neighboring -Z residue at the C-terminus may at least partially account for an apparent decrease in $\Delta(\Delta G^\circ)_{\text{gly}}$ with increasing peptide length, as reported by Mayer et al. [9] since the first gly residue contribution would have a neighboring -OH at its C-terminus and a larger $\Delta(\Delta G^\circ)_{\text{gly}}$ of ~4.4 kcal/mol (as also reported by Mayer et al.) while subsequent gly residues would be flanked by -CONH- at $i + 1$ and therefore exhibit reductions in $\Delta(\Delta G^\circ)_{\text{gly}}$ to ~3 kcal/mol. Overall, comparisons within the RGZ/RZ series of compounds show a substantial reduction of up to 2−4 kcal/mol in the energetic penalty for insertion of the peptide backbone amide bond into bilayers depending on the -Z residue. Significant nonadditivity in $\Delta(\Delta G^\circ)_{\text{gly}}$ exists, which appears to be due largely to the impact of variations in the -Z substituent.

Development of a New LFER for Lipid Bilayer Permeability. The ultimate aim of developing a new LFER for lipid bilayer transport was to enable the prediction of permeability solely from permeant structure and bilayer composition. Fragment-based methods are most attractive in this regard since they require no physicochemical property data or any other information about the permeant other than its structure. The proximity effects identified above in the determination of $\Delta(\Delta G^\circ)_{\text{gly}}$ from the RGZ/RZ series of compounds indicate that any attempt to develop an LFER to account for the lipid bilayer permeability coefficients of peptides must take into account the effects of neighboring polar residues. Also, since partition coefficient data as well as permeability data are available, a relationship that could incorporate both data sets would be desirable. Structure−transport relationships based on partitioning data may become more valuable as research is extended beyond the liquid crystalline, single component bilayers comprised of egg-PC or DOPC explored in this study to more complex and highly ordered membranes.

Selection of a Relevant Hydropathy Scale for Predicting Permeability Coefficients. Most commonly, solvation or hydropathy scales based on partitioning of model peptides between water and 1-octanol[26,29,31,37] are employed to account for membrane binding of peptides, while the transport of polar permeants such as peptides across liquid crystalline lipid bilayers correlates best with hydrocarbon/water partition coefficients.[5,7–9,11,13] This apparent conflict is understandable if one considers that the region of a bilayer membrane probed in a membrane-binding experiment is the interfacial region while the barrier domain in lipid bilayers is the hydrocarbon chain region. The partitioning data in Tables 1 and 2 and in Figure 4 demonstrate that 1-octanol/water partition coefficients are much less selective to solute polarity than 1,9-decadiene/water partition coefficients, which more closely resembles the selectivity of the barrier domain of egg PC or DOPC. These differences reflect primarily the ability of octanol to form hydrogen bonds with the solute while this is not possible in hydrocarbon solvents. From the standpoint of chemical selectivity, therefore, transfer free energies, $\Delta(\Delta G^\circ)_x$, obtained from decadiene/water partitioning data are predictive of relative bilayer permeabilities, providing that permeant size does not vary.

Correction for the Effect of Permeant Size on Lipid Bilayer Permeability. A careful examination of the transfer free energies in Table 3 reveals significant differences in $\Delta(\Delta G^\circ)_x$ values obtained from permeability coefficients compared to those obtained from partitioning data. Generally, $\Delta(\Delta G^\circ)_x$ values obtained from permeability coefficients are up to several hundred calories more positive (i.e., transport is less favorable than predicted from bulk solvent/water partition coefficients alone), indicating a systematic bilayer effect on the transport of these model compounds.

Previous studies in this and other laboratories[11,15–17,19,40] have demonstrated that chain ordering in lipid bilayers imposes an additional barrier to lipid bilayer transport, which may reflect solute exclusion from the ordered chain region as well as effects on the diffusion coefficient due to chain ordering.[14,44–46] Thus, the classical bulk-solubility diffusion model for lipid bilayer permeability which is based solely on assumptions valid in bulk solvents must be modified. The barrier-domain model for bilayer permeability first proposed by Xiang and Anderson corrects the permeability coefficient predicted from the bulk solubility-diffusion model, P_o, for the effects of chain ordering using a permeability decrement correction factor, f, (i.e., $P = fP_o$) that

(44) Xiang, T.-X. Translational diffusion in lipid bilayers: Dynamic free-volume theory and molecular dynamics simulation. *J. Phys. Chem. B.* **1999**, *103*, 385–394.

(45) Xiang, T.-X.; Anderson, B. D. Molecular distributions in interphases: A statistical mechanical theory combined with molecular dynamics simulation. *Biophys. J.* **1994**, *66*, 561–573.

(46) Xiang, T.-X.; Anderson, B. D. Molecular dissolution processes in lipid bilayers: A molecular dynamics simulation. *J. Chem. Phys.* **1999**, *110*, 1807–1818.

depends both on bilayer composition (i.e., the chain ordering) and permeant size.[17,19]

Xiang and Anderson[15] established empirically that the logarithm of permeability coefficient for a series of permeants in egg PC bilayers normalized by the decadiene/water partition coefficient was linearly dependent on the logarithm of the permeant molecular volume, with a slope (−1.4) that was amplified over that for diffusion in the bulk hydrocarbon decane. Based on this observation, the following equation was employed to account for the dependence of permeability on permeant volume

$$\ln\frac{P}{\mathrm{PC}} = \ln\frac{D_0}{\delta} - n\ln V$$

where V is the molecular volume of the compound of interest and n represents the size selectivity parameter. The equation can be transformed to free energy format

$$\Delta G^{\circ}(P) - \Delta G^{\circ}(\mathrm{PC}) = RT\ln\frac{\delta}{D_0} + nRT\ln V$$

where $\Delta G°(P)$ and ΔG °(PC) are the total transfer free energies of a given compound obtained from permeability and partition coefficients, respectively, and $RT\ln(\delta/D_0)$ is a constant.

Using formic acid as the reference compound, the above equation can be rearranged to

$$\Delta(\Delta G^{\circ})_x(P) - \Delta(\Delta G^{\circ})_x(\mathrm{PC}) = nRT\ln\frac{V_{\mathrm{sub}}}{V_{\mathrm{ref}}}$$

where V_{sub} and V_{ref} are the molecular volumes for the substituted and reference compound (formic acid).

Nonlinear regression analysis according to eqs 9 and 11 for all model compounds in Table 3 generated a size selectivity parameter (n) of 0.84 (Table 4) with a 95% confidence interval of 0.34−1.35. This confidence range establishes the necessity of making the size correction and overlaps with that previously observed for egg PC bilayers using a different permeant set.[15] The size selectivity parameter depends on chain ordering. Thus, the value of n would be expected to increase significantly in highly ordered membranes such as those in their gel phase at 25 °C.

Nonpolar Surface Area, σ_{np}, and the Selectivity of the Bilayer Barrier Domain to Nonpolar Residues. A substantial body of literature has established that the selectivity of organic solvents to nonpolar residues (e.g., alkyl groups, etc.) does not differ greatly, with reported values of σ_{np} obtained from bulk solvent/water partition coefficients ranging from −18.9 to −25 cal/mol/Å^2.[30,47–51] Thus, literature values of −22.8 and −20.9 cal/mol/Å^2 (Table 4) determined from the octanol/water partitioning of peptides as reported by Wimley et al.[30,51] are similar to the result of −21.2 cal/mol/Å^2 obtained in this study for partitioning into decadiene or the barrier domain of liquid crystalline egg PC or DOPC bilayers. However, in the same research, Wimley reported a much lower σ_{np} (−13.9 cal/mol/Å^2) for interfacial binding of amino acids to phospholipid bilayers, indicating that binding experiments probe a different region of bilayers, a region that is distinctly more water-like than the barrier domain.

Wimley et al. reported surface areas of 42 and 80 Å^2 for the alkyl portions of glycine and alanine residues in Ac-GG-x-GG peptides,[30] and Eisenberg et al.[37] also provided a similar value (40 Å^2) for the -CH_2- group in glycine. The values obtained in the present study for the surface areas of the backbone -CH_2- in a glycine residue and the alkyl group in alanine were 39 ± 4 and 73 ± 0.3 Å^2, respectively, both of which are in reasonable agreement though slightly smaller than those reported previously.

Walter and Gutknecht generated a methylene group contribution of −764 ± 54 cal/mol to the apparent free energy of permeant transfer into the barrier domain of egg lecithin bilayers from permeability coefficients of aliphatic monocarboxylic acids.[43] If σ_{np} (−21.2 cal/mol/Å^2) is multiplied by the A_{np} of 35 Å^2 obtained in this study for the surface area of the -CH_2- group in a linear aliphatic chain a value of −740 cal/mol is obtained, in close agreement with the value previously reported.

Free Energy Contributions of Polar Groups and Correction Factors for Backbone Amide Bonds. The newly generated polar parameters ($\Delta(\Delta G°)_P$), such as -COO-, -CON<, -O-, and related hydrogens, along with the neighboring $i + 1$ residue correction factors that are applied to each peptide backbone amide are listed in Table 4. As previously demonstrated in the RGZ/RZ series of peptides, significant, neighboring residue dependent self-solvation of the peptide backbone amide occurs with -O- containing $i + 1$ residues accounting for a 1.8 kcal/mol reduction in the free energy penalty for transferring an amide backbone from water to decadiene or the barrier domain of an egg PC or DOPC lipid bilayer while -N- containing $i + 1$ residues account for a 2.6−3.4 kcal/mol reduction.

The fragment constants in Table 4 can be combined to construct other polar functional group contributions, such as the contribution for insertion of a glycyl residue adjacent to a neighboring ($i + 1$) -COOH group, by the following equations using parameters in Table 4:

$$\Delta(\Delta G^{\circ})_{\mathrm{gly(-COOH)}} = \Delta(\Delta G^{\circ})_{\mathrm{-CON<}} + \Delta(\Delta G^{\circ})_{\mathrm{-H(first)}} + \sigma_{np}\Delta A_{np} + \Delta(\Delta G^{\circ})_{\mathrm{corr(-COOH)}}$$

$$\Delta(\Delta G^{\circ})_{\mathrm{gly-(-COOH)}} = 6568 + 357 + (-21.2)39 + (-1780) \approx 4300\ \mathrm{cal/mol}$$

The predicted value (4.3 kcal/mol) matches the values reported from both the RGZ/RZ and Tol- series of compounds as shown in Table 5.

(47) Chothia, C. Hydrophobic bonding and accessible surface area in proteins. *Nature (London)* **1974**, *248*, 338–339.
(48) Nozaki, Y.; Tanford, C. The solubility of amino acids and two glycine peptides in aqueous ethanol and dioxane solutions. *J. Biol. Chem.* **1971**, *246*, 2211–2217.
(49) Reynolds, J. A.; Gilbert, D. B.; Tanford, C. Empirical correlation between hydrophobic free energy and aqueous cavity surface area. *Proc. Natl. Acad. Sci. U.S.A.* **1974**, *71*, 2925–2927.
(50) Rose, G. D.; Geselowitz, A. R.; Lesser, G. J.; Lee, R. H.; Zehfus, M. H. Hydrophobicity of amino acid residues in globular proteins. *Science* **1985**, *229*, 834–838.
(51) Wimley, W. C.; White, S. H. Experimentally determined hydrophobicity scale for proteins at membrane interfaces. *Nat. Struct. Biol.* **1996**, *3*, 842–848.

Table 5. Comparison of the Transfer Free Energies of Amino Acid Residues (gly, ala, and sar) with Various Neighboring ($i + 1$) Substituents Obtained from Different Series of Compounds

	current LFER[a]	RGZ/RZ series	Tol- series
peptide residues ($i + 1$ substituent)	$\Delta(\Delta G^\circ)$x (cal/mol)	$\Delta(\Delta G^\circ)$x (cal/mol)	$\Delta(\Delta G^\circ)$x (cal/mol)
-Gly-(-COOH)	4.3	4.1	4.6
-Gly-(-CONH-)	3.4	3.1	
-Gly-(-CONMe-)	2.7	2.4 ~ 2.8	
-Ala-(-COOH)	3.6		3.6

isolated groups (Rx/RH) -x	$\Delta(\Delta G^\circ)$x (kcal/mol)	$\Delta(\Delta G^\circ)$x (kcal/mol) p-Toluic acid[b] or pTAA[d]	$\Delta(\Delta G^\circ)$x (kcal/mol) p-Methylhippuric acid[c]
-Cl	0.1	0.3	0.2
-OCH_3 (ether)	0.8	0.7	0.9
-CN	2.1	2.2	2.4
-OH	4.0	3.9	4.0
-COOH	5.1	5.2	4.7
-CONH2	5.6	6.1	6.4
-CONHMe	6.1	5.8[d]	
-CONMe2	4.9	4.5[d]	

[a] Using Table *4* with formic acid as the reference compound. [b] From Xiang and Anderson[13] [c] From Mayer et al.[7] [d] From Mayer et al.[9]

Transfer free energies of well-isolated polar functional groups (e.g., -COOH, -COOMe, -CONHMe, etc.) typically generated by comparing transfer free energies of a substituted compound (RX) to an unsubstituted reference compound (RH) have been reported in previous publications from these laboratories using *p*-toluic acid, *p*-methylhippuric acid, and *p*-tolylacetic acid as reference compounds.[7,9,13] For polar substituents attached to the *p*-CH_3- group in these compounds, the group contributions reported reflected both the addition of -X and the removal of -H from the terminal -CH_3 group. In order to compare the fragment-based predictions from the present method with those previously reported values, the contribution for removal of a methyl hydrogen must be included in the fragment-based LFER estimation. The A_{np} for one of the hydrogen atoms from the *p*-methyl group in *p*-toluic acid and *p*-methylhippuric acid was estimated from the nonpolar surface area differences of CH_3-C_6H_4-/-CH_2-C_6H_4- acid pairs (Table 3) to be 43.4 Å^2, resulting in a free energy contribution of 0.9 kcal/mol. Thus, the fragment constant for the contribution of X = -CONHMe attached to a terminal -CH_3 on *p*-toluic acid would be obtained as follows

$$\Delta(\Delta G^\circ)_{-\mathrm{CONHMe}} = \Delta(\Delta G^\circ)_{-\mathrm{CON<}} + \Delta(\Delta G^\circ)_{-\mathrm{H(first)}} + \sigma_{np}\Delta A$$

$$\Delta(\Delta G^\circ)_{-\mathrm{CONHMe}} = 6568 + 357 + (21.2)(81.4-43.4) \approx 6100 \text{ kcal/mol}$$

where ΔA_{np} is the difference between the nonpolar surface area for the amide methyl grouparea for the amide methyl group (81.4 ± 0.8 Å^2 obtained by comparing MPA-NHMe to MPA-OH or MPA-G-NHMe/MPA-G-OH) and a methyl hydrogen. The corrected $\Delta(\Delta G^\circ)_x$ from the current LFER and the previously published values listed in Table 5 show reasonable agreement.

The parameters in Table 4 may also be used to predict permeability and decadiene/water partition coefficients from eqs 10 and 12. Thus, for Tol-G

$$PC = 6.2\times10^{-4}\exp[-(\sigma_{np}\Delta A_{np} + \Delta(\Delta G^\circ)_{-\mathrm{CON<}} + \Delta(\Delta G^\circ)_{-\mathrm{H(first)}} + \Delta(\Delta G^\circ)_{\mathrm{corr(-COOH)}})/RT]$$

and

$$P = 2.9\times10^{-3}\exp[-(nRT\ln(V_{sub}/V_{ref}) + \sigma_{np}\Delta A_{np} + \Delta(\Delta G^\circ)_{-\mathrm{CON}} + \Delta(\Delta G^\circ)_{-\mathrm{H(first)}} + \Delta(\Delta G^\circ)_{\mathrm{corr(-COOH)}})/RT]$$

where $\Delta A_{np} = 248.5 - 27.8 = 220.7$ Å^2; The predicted PC and *P* of Tol-G are 2.82×10^{-4} and 3.72×10^{-4} cm/s, which are in good agreement with the experimental values listed in Table 3 for both PC (3.4×10^{-4}) and *P* (4.9×10^{-4} and 6.4×10^{-4} cm/s), respectively.

Possible Reasons for the Observed Nonadditivity of $\Delta(\Delta G^\circ)_{\text{-CONH-}}$. The significant influence that $i + 1$ neighboring residues exert on the free energy of transfer of a backbone amide from water to decadiene or the barrier domain of an egg PC or DOPC lipid bilayer may be the result of intramolecular hydrogen bonding or nonspecific proximity effects related to differences in solvation or internal electrostatic interactions induced by the flanking residue. As shown in numerous studies,[52–56] even small peptides exhibit conformation-dependent intramolecular hydrogen bonding. Recent FTIR and NMR studies indicate that single residue peptides varying in their C-terminus, including Ac-G-NMe_2, adopt not only a stretched conformation in CCl_4, but also exhibit 5-membered ring formation (i.e., a C_5 conformation) suggesting an intramolecular hydrogen bond (gly -NH--*O*=C) [55,57,58] in which the terminal -C=O and amide -NH are virtually parallel to each other such that their interaction may limit free rotation. Several computational studies indicate that C_5 and C_7 (HB between terminal -NH or -OH and inner *C*=O) conformations may coexist in very simple peptides.[59,60]

(52) Mizushima, S.; Shimanogouchi, T.; Tsuboi, M.; Arakawa, T. Near infrared spectra of compounds with two peptide bonds and the configuration of a polypeptide chain. VI. Further evidence of the internal hydrogen bonding and the estimation of its energy. *J. Am. Chem. Soc.* **1957**, *39*, 5357–61.

(53) Toniolo, C.; Palumbo, M.; Benedetti, E. On the oxy analogues to the 3→1 intramolecularly hydrogen-bonded peptide conformations. *Macromolecules* **1976**, *9*, 420–424.

(54) Madison, V.; Dopple, K. D. Solvent-dependent conformational distributions of some dipeptides. *J. Am. Chem. Soc.* **1980**, *102*, 4855–4863.

(55) Neel, J. Experimental study of the influence of specific intramolecular interactions on the conformation of model molecules. (Peptides and oligopeptides). *Pure Appl. Chem.* **1972**, *31*, 201–225.

(56) Madison, V.; Delaney, N. G. Thermodynamics of solvation for methylproline peptides. *Biopolymers* **1983**, *22*, 869–877.

(57) Plass, M.; Griehl, C.; Kolbe, A. Solvent effect on the conformational behavior of amino acid and oligopeptide derivatives. *J. Mol. Struct.* **2001**, *570* (1–3), 203–214.

(58) Ashish; Kishore, R. Thermodynamic characterizations of an intramolecularly hydrogen bonded C5-structure across proteinogenic residue. *FEBS Lett.* **1997**, *417* (1), 97–100.

Madison and Delaney[56] concluded that differences in the free energies of transfer of *syn*- and *anti*-Ac-3-Me-ProNHMe from carbon tetrachloride to water could be attributed to differences in the fractions of intramolecular hydrogen bonded C_7 conformer in the organic phase.

Intramolecular hydrogen bonding in small peptides is highly sensitive to the solvent, being increasingly favored in less polar environments.[54,61,62] Recent molecular dynamics simulations of small alanine-containing peptides (*p*-toluyl-Ala_n ($n = 0-3$)) in CCl_4 and water revealed that their preferred conformation depended strongly on the solvent, with folded conformations (5- and 7-membered rings) dominating in CCl_4.[62] The formation of folded structures was found to partially compensate for the loss of water of solvation during peptide transfer from water to CCl_4 thus facilitating peptide transfer in comparison to that expected in the absence of intramolecular hydrogen bond formation. Solvent-induced changes in intramolecular hydrogen bonding and the accompanying changes in peptide conformation have been referred to as the "chameleon effect".[63,64]

Ester substitution has been frequently utilized in studies of intramolecular hydrogen bonding in peptides and proteins due to the structural similarities of ester and amide bonds in terms of their planarity, preference for trans conformations, and similar bond angles and lengths.[65] The ester carbonyl is a weaker hydrogen acceptor than the amide carbonyl, however, and replacement of amide linkages with esters typically results in decreases in protein stability.[65–71] These observations combined with the differential effects of -O- versus -N-containing flanking residues on the backbone amide free energies of transfer found in this study make plausible the argument that variations in the $i + 1$ residue correction term may reflect alterations in the impact of adjacent residues on intramolecular hydrogen bonding. However, the present studies do not rule out other factors that may also contribute to the observed proximity effects.

Comparing the values of $\Delta(\Delta G^\circ)_{gly}$ generated by partitioning RGZ/RZ compounds in different solvent systems could potentially shed light on the significance of hydrogen bonding to the nonadditive contributions of peptide backbone and amino residues. The results obtained from the partitioning experiments conducted in 1-octanol/water and CCl_4/water along with decadiene/water are depicted in Table 2 and Figure 4. These results show a trend, similar to the one obtained from decadiene/water, that $\Delta(\Delta G^\circ)_{gly}$ obtained from RGZ/RZ compounds with an oxygen-based C-terminus is higher than $\Delta(\Delta G^\circ)_{gly}$ obtained from the compounds with a nitrogen-based C-terminus. In CCl_4/water, the difference between the average values of these two categories is 1.8 kcal/mol, which is comparable to that obtained from decadiene/water while the absolute values of $\Delta(\Delta G^\circ)_{gly}$ are lower than those in decadiene/water. In 1-octanol/water, the absolute values of $\Delta(\Delta G^\circ)_{gly}$, are considerably lower than those in CCl_4/water and 1,9-decadiene/water and the $\Delta(\Delta G^\circ)_{gly}$ difference between RGOMe/ROMe and $RGNMe_2$/$RNMe_2$ diminishes from 1.7−1.8 kcal/mol in CCl_4/water or 1,9-decadiene/water to 0.5 kcal/mol in 1-octanol/water. The tendency of solutes to form intramolecular hydrogen bonds should be reduced in 1-octanol, which is well-known as a hydrogen bonding solvent. Overall the solvent dependence of $\Delta(\Delta G^\circ)_{gly}$ provides further evidence for the hypothesis that intramolecular hydrogen bonding, which is reduced in a hydrogen bonding solvent, could be an important contributor to the $i + 1$ residue dependent nonadditivity in $\Delta(\Delta G^\circ)_{gly}$.

Conclusions

Careful examinations of a series of RGZ/RZ compound pairs showed substantial effects of the $i + 1$ residue on the free energy contribution of the peptide backbone amide in

(59) Fraternali, F.; Van Gunsteren, W. F. Conformational transitions of a dipeptide in water: Effects of imposed pathways using umbrella sampling techniques. *Biopolymers* **1994**, *34*, 347–355.
(60) Shang, H. S.; Head-Gordon, T. Stabilization of helixes in glycine and alanine dipeptides in a reaction field model of solvent. *J. Am. Chem. Soc.* **1994**, *116* (4), 1528–32.
(61) Eker, F.; Cao, X.; Nafie, L.; Huang, Q.; Schweitzer-Stenner, R. The structure of alanine based tripeptides in water and dimethyl sulfoxide probed by vibrational spectroscopy. *J. Phys. Chem. B* **2003**, *107*, 358–365.
(62) Xiang, T.-X.; Anderson, B. D. Conformational structure, dynamics and solvation energies of small alanine peptides in water and carbon tetrachloride. *J. Pharm. Sci.* **2006**, *95*, 1269–1287.
(63) Carrupt, P.-A.; Testa, B.; Bechalany, A.; El Tayar, N.; Descas, P.; Perrissoud, D. Morphine 6-glucuronide and morphine 3-glucuronide as molecular chameleons with unexpected lipophilicity. *J. Med. Chem.* **1991**, *34*, 1272–1275.
(64) El Tayar, N.; Mark, A. E.; Vallat, P.; Brunne, R. M.; Testa, B.; Van Gunsteren, W. F. Solvent-dependent conformation and hydrogen-bonding capacity of cyclosporin A: Evidence from partition coefficients and molecular dynamics simulations. *J. Med. Chem.* **1993**, *36*, 3757–3764.
(65) Beligere, G. S.; Dawson, P. E. Design, synthesis, and characterization of 4-ester CI2, a model for backbone hydrogen bonding in protein α-helices. *J. Am. Chem. Soc.* **2000**, *122* (49), 12079–12082.
(66) Thorson, J. S.; Chapman, E.; Schultz, P. G. Analysis of hydrogen bonding strengths in proteins using unnatural amino acids. *J. Am. Chem. Soc.* **1995**, *117* (36), 9361–2.
(67) Chapman, E.; Thorson, J. S.; Schultz, P. G. Mutational analysis of backbone hydrogen bonds in staphylococcal nuclease. *J. Am. Chem. Soc.* **1997**, *119* (30), 7151–7152.
(68) Koh, J. T.; Cornish, V. W.; Schultz, P. G. An experimental approach to evaluating the role of backbone interactions in proteins using unnatural amino acid mutagenesis. *Biochemistry* **1997**, *36* (38), 11314–11322.
(69) Shin, I.; Ting, A. Y.; Schultz, P. G. Analysis of backbone hydrogen bonding in β-turn of staphylococcal nuclease. *J. Am. Chem. Soc.* **1997**, *119* (51), 12667–12668.
(70) Haque, T. S.; Little, J. C.; Gellman, S. H. Stereochemical requirements for β-hairpin formation: Model studies with four-residue peptides and depsipeptides. *J. Am. Chem. Soc.* **1996**, *118* (29), 6975–6985.
(71) Wales, T. E.; Fitzgerald, M. C. The energetic contribution of backbone-backbone hydrogen bonds to the thermodynamic stability of a hyperstable P22 arc repressor mutant. *J. Am. Chem. Soc.* **2001**, *123* (31), 7709–7710.
(72) Hansch, C.; Leo, A.; Hoekman, D. Exploring QSAR: Volume 2: Hydrophobic, Electronic, and Steric Constants. **1995**,

studies of partitioning between water and various organic solvents and studies of permeability through DOPC bilayers. Compounds having-CONHMe and -$CONMe_2$ C-termini substantially reduced the $\Delta(\Delta G°)_{\text{-CONH-}}$ compared to compounds with -COOH or -COOMe termini. Permeability (DOPC or egg-PC) and partition coefficients (decadiene/water) for a series of 47 model compounds were compiled to construct a comprehensive, fragment-based linear free energy relationship to predict passive permeability of small peptides and simple organic molecules across DOPC (egg PC) bilayers. The new LFER analysis is applicable only to lipid bilayer permeability in relatively disordered bilayers (i.e., liquid crystalline bilayers at room temperature) since the size dependence of permeability coefficients are highly sensitive to chain ordering. Also, use of the model for more complex peptides beyond those containing glycine, alanine, or sarcosine amino acid residues has not been validated. Peptides containing amino acids having hydrogen donor or acceptor functional groups in their side chains present another level of complexity that would have to be systematically addressed before the LFER approach could be extended to such molecules.

Acknowledgment. We thank Dr. Sagar Rane for his help and important discussions of this work.

MP700100N